Influence of future CO_2 concentrations on growth and nitrogen fixation in the bloom-forming cyanobacterium *Nodularia spumigena*

Diplom thesis

by

Jan Czerny

Supervisor:

Prof. Dr. Ulf Riebesell

Kiel, January 2008

Christian Albrechts-Universität zu Kiel

Mathematisch-Naturwissenschaftliche Fakultät

Abstract

Besides the well-known atmospheric climate change, anthropogenic CO_2 emissions are resulting in elevated CO_2 concentrations and acidification in the surface ocean. Phytoplankton physiological responses to these chemical alterations are influencing ocean primary production and thus the fixation of CO_2 and its transport into deep waters. Diazotrophic cyanobacteria play a special role in this process since they are able to provide the ecosystem with nitrogen; the nutrient limiting primary production in most of the ocean regions. Future changes in carbon and nitrogen fixation can influence the ocean in its function as the most important sink for anthropogenic CO_2.

Stimulating effects of elevated [CO_2] on carbon fixation have been observed in eukaryotic and prokaryotic phytoplankton species as well as in natural phytoplankton assemblages. For the non-heterocystic oceanic cyanobacterium *Trichodesmium* it was shown that not only carbon fixation but also nitrogen fixation rates rise in response to high [CO_2]. Whether this is a general pattern in diazotrophic cyanobacteria is unknown. This study shows that *Nodularia spumigena*, an important heterocystic bloom forming cyanobacterium of the Baltic Sea, reacts to elevated [CO_2] and corresponding acidification as projected for the year 2100 with strongly impeded growth and reduced nitrogen fixation. These effects were accompanied by storage of nutrients and significant changes in the elemental composition of the cells. Carbon and phosphorus cellular content increased about twice as much under high [CO_2] than cellular nitrogen content.

Findings of impeded growth of *N. spumigena* under lowered ambient pH are contrasting the findings in marine phytoplankton but show similarities to several studies on heterocystic bloom forming cyanobacteria in freshwater. Aggregation and the formation of surface scums are typical for blooms of *N. spumigena* and its freshwater relatives. Regarding the preference for high pH *N. spumigena* is hypothesized to be adapted to a microclimate caused by photosynthetic activity under high growth densities. However, as the cyanobacterial filaments are initially suspended in the water column, first aggregation and bloom development of *N. spumigena* will probably be delayed under future [CO_2] and pH.

Zusammenfassung

Neben den allseits bekannten Auswirkungen auf das atmosphärische Klima bewirkt der Ausstoß von CO_2 durch den Menschen steigende CO_2 Konzentrationen und fortschreitende Ansäuerung im Oberflächenozean. Physiologische Reaktionen des Phytoplanktons auf diese chemischen Veränderungen können sich auf die biologische Produktivität und somit auf die Fixierung von CO_2 und dessen Transport in Tiefenwasser auswirken. Durch ihre Fähigkeit atmosphärischen Stickstoff biologisch verfügbar zu machen, nehmen diazotrophe Cyanobakterien unter den meist Stickstoff limitierten Primärproduzenten eine Sonderrolle ein. Zukünftige Veränderungen in ozeanischer Kohlenstoff- und Stickstofffixierung könnten weit reichende Auswirkungen auf die Funktion des Ozeans als die wichtigste Senke für anthropogenes CO_2 haben.

Erhöhte CO_2 Konzentrationen haben sich in Experimenten förderlich auf die Kohlenstofffixierung in eukaryotischen und prokaryotischen Phytoplanktonkulturen sowie natürlichen Phytoplanktongemeinschaften ausgewirkt. An dem ozeanischen nicht-heterocystischen Cyanobacterium *Trichodesmium* wurde gezeigt, dass nicht nur Kohlenstoff- sondern auch Stickstofffixierung durch erhöhte CO_2 Konzentrationen gefördert werden kann. Ob es sich bei dieser Beobachtung um ein generelles physiologisches Muster bei diazotrophen Cyanobakterien handelt, das sich auch auf Phytoplanktongemeinschaften in Randmeeren und Estuaren übertragen lässt, ist nicht bekannt. Die Ergebnisse dieser Studie zeigen, dass *Nodularia spumigena*, ein wichtiges blütenbildendes Cyanobakterium der Ostsee, auf eine Erhöhung der CO_2 Konzentration und die damit verbundene Ansäuerung, wie sie für das Jahr 2100 erwartet werden, mit stark verlangsamten Wachstum und verminderter Stickstofffixierung reagiert. Diese Effekte wurden durch die Speicherung von Nährstoffen und starke CO_2 bedingte Veränderungen in der elementaren Zusammensetzung der gebildeten Biomasse begleitet. Kohlenstoff und Phosphor sammelten sich mit steigendem [CO_2] in den Zellen doppelt so stark an wie Stickstoff.

Der Befund eines negativen Zusammenhangs von CO_2 Konzentrationen und Biomassezuwachs bei *N. spumigena* steht im direkten Gegensatz zu den auf bisherigen Erkenntnissen aus marinem Phytoplankton beruhenden Erwartungen. Ein negativer Einfluss von erniedrigten pH-Werten auf die Entwicklung blütenbildender heterocystischer Cyanobakterien in limnischen Habitaten ist allerdings allgemein bekannt. Aggregation und das Bilden von Oberflächenbelägen ist typisch für *N. spumigena* und ihre limnische Verwandtschaft. Ähnlich den Süßwasserformen ist *N. spumigena* wahrscheinlich an das

basische, durch Primärproduktion in hohen Wachstumsdichten gebildete, Mikroklima angepasst. Da die Cyanobakterienfäden allerdings zunächst verteilt im Wasser vorliegen, wird sich wahrscheinlich Aggregation und Blütenentwicklung unter zukünftigen CO_2 und pH Bedingungen verzögern.

Index

1. Introduction

1.1. Prologue

Since the beginning of the industrialization, humans dramatically change the Earth's atmosphere due to massive emissions of greenhouse gases by burning fossil biomass. This leads to a multitude of sudden changes to an environment that was slowly formed by interactions and feedbacks of physicochemical, geological and biological processes over the last 3.5 billion years.

One key question in science today is how the system earth will react to the future changes. It is a question of immense complexity that demands unprecedented collaboration of numerous scientific disciplines.

The ocean, as it covers more than 2/3 of our planet's surface, plays a major role in global cycling of energy and matter. Interacting physical, chemical and biological processes in the ocean yielded an uptake of about half of the anthropogenic carbon dioxide produced in the last two centuries.

To what extent has the ocean the capacity to intercept global change? And at what ecological expense?

Especially the biological processes and their responses to the changing environment are a major source of uncertainty in global estimates for future CO_2 uptake of the ocean. Midget differences in the physicochemical environment can lead to substantial changes in the marine life of ocean regions.

This study investigates the response of a dominant bloom forming cyanobacterial species of the Baltic Sea to a changing factor: Increasing atmospheric CO_2 concentrations. In the context of further investigations it could serve as a small piece of the puzzle for understanding the reaction of the Baltic ecosystem to changes in CO_2 concentrations and corresponding acidification.

1.2. Climate change and ocean acidification

1.2.1. Anthropogenic climate change

Atmospheric concentrations of the major greenhouse gases CO_2 and methane seem to be directly coupled with temperature and have been oscillating in phase with it during at least the last 420,000 years (Petit et al. 1999). CO_2 concentrations between 180 ppm and 280 ppm and associated temperature changes of 10 °C, recorded in Antarctic ice cores are considered as characteristics of glacial and interglacial periods (Siegenthaler et al. 2005). These fluctuations, as well as the small-scale fluctuations of the last millennium were always stabilised by feedback mechanisms with the biosphere (Indermuehle et al. 1999) that coevolved with the atmosphere (Kasting and Siefert. 2002).

Since the beginning of industrialisation, atmospheric concentrations of greenhouse gases increased at an extraordinary rate, mainly as a result of the combustion of fossil fuel. Interestingly, estimates for global warming of 6 °C for a doubling of atmospheric CO_2 concentration by Arrhenius (1896) are not far from present estimates.

From an interglacial level of 280 ppm in preindustrial times, (Indermuehle et al. 1999) concentrations of 380 ppm have already been reached (Keeling and Whorf 2005) and the present value is expected to double by the end of the century (Figure 1a). Today, some effects of this alteration of the atmosphere can already be observed and others can be expected in the next millennium. Observed global warming (Jones and Moberg. 2004) and secondary effects like sea level rise and the melting of the polar ice caps (Christoffersen and Hambrey. 2006; Otto-Bliesner et al. 2006), can already be accredited to human activity with a certainty of more than 90% (Forster et al. 2007).

The understanding of feedback mechanisms that could attenuate or intensify climate change is still in its infancy.

1.2.2. Anthropogenic CO_2 in the ocean

CO_2 is a polar molecule that is not only of high solubility but also reacts with water molecules according to the following equations:

$$CO_2 + H_2O \Leftrightarrow H^+ + HCO_3^-$$

$$HCO_3^- \Leftrightarrow H^+ + CO_3^{2-}$$

The resulting protons from these reactions immediately react with anions present in seawater. Subsequent reactants are mainly carbonate and bicarbonate (95%) but also the boric acid anion ($B(OH)^{4-}$), hydroxide (OH^-) and many other anions of minor concentration. The sum of protons that can be taken up by these anions is called "Total Alkalinity". The sum of the concentrations of all carbon species in this equilibrium is termed Dissolved Inorganic Carbon [DIC].

Despite the great buffering capacity, the pH of the surface ocean has already decreased by ~0.1 units due to the uptake of anthropogenic CO_2 and is expected to fall further 0.3 to 0.4 units until the end of this century (under a IS92a Scenario)(Meehl et al. 2007) (Figure 1b).

At current pH (~8.1) dissolved CO_2 accounts for less than 1% of DIC. Future increase in pH will lead to successive protonation of the other carbon species and will shift the equilibrium towards higher CO_2 and lower CO_3^{2-} concentrations, thus lowering the oceanic uptake capacity for further CO_2 (Feely et al. 2004). Due to global warming future uptake of CO_2 will be additionally impeded by the reduction of gas solubility and mixing (Friedlingstein et al. 2006). A measure of the buffer capacity of sea water for the uptake of CO_2 is the Revelle factor which is defined as the ratio of the change in pCO_2 per change in [DIC] versus the actual pCO_2 per [DIC] (Takahashi 2004).

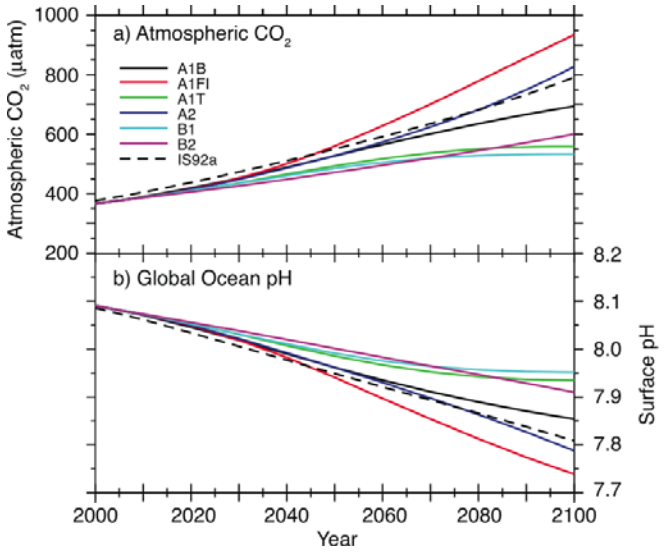

Figure 1: Atmospheric CO_2 partial pressure (a) global ocean pH (b) as projected in seven different emission scenarios (modified after IPCC 2007).

Because of thermal stratification, the top layer of the ocean that is in contact with the atmosphere is relatively small and strongly affected by atmospheric CO_2 concentrations increasing so much faster than the ocean mixing time (~1,000 years).

Within the Baltic Sea total DIC, salinity and alkalinity is lower compared to ocean values due to a strong riverine influence in this marginal sea. As a result of that and of a high biological productivity its carbonate system shows a much stronger seasonal variability than that of the open ocean concerning the concentrations of total inorganic carbon as well as of CO_2 (Thomas and Schneider 1999). Furthermore, acidic rain causes a significant additional acidification effect in coastal seas like the Baltic (Doney et al. 2007).

The ocean represents a vast reservoir of dissolved inorganic carbon, approximately 50 times larger than the atmospheric reservoir. Thus it has the potential to absorb much of the anthropogenic CO_2. By 1994, the ocean had already taken up about half of the CO_2 emitted since the beginning of the industrialisation (118 ± 19 out of 244 ± 20 Pg since 1800). So it will be able to take up ~90 % of it after complete equilibration (Sabine et al. 2004). However, it will take several thousand years for the ocean to mix sufficiently to do so (Archer 2005).

Apart from the different physical ocean mixing processes, the only other natural path for carbon to enter the ocean interior is by the sinking of biogenic particles from the surface layer. This process is commonly referred to as the biological carbon pump. It accounts for the transport of ~8-12 Pg of the total marine annual primary production of ~45 Pg (Oschlies 2001) into deeper water layers. This sink of atmospheric carbon is nearly balanced by the release of CO_2 by the ocean in regions were oversaturated water from deep layers reaches the surface and equilibrates. The net result is a current uptake of only ~2 Pg per year (Takahashi 2004).

The performance of the biological pump does not directly depend on the annual primary production of the oceans, but to a great extent on the sinking properties of the formed particles. Therefore it is thought to be highly sensitive to cell dimensions, ballast, aggregation potential and growth density of the dominant phytoplankton as well as to the type of grazers that feed upon it (Ittekot 1996). The amount and composition of biomass produced is mostly triggered by nutrient supply. Changes in nutrient supply by a climate-induced increase of ocean stratification and consequent changes in ocean productivity are roughly quantified (Sarmiento et al. 2004). However, ecological responses to climate change are a major source of uncertainty (Laws et al. 2000). Processes that affect primary production, like nitrogen fixation (Mahaffey et al. 2005), and export of organic carbon, like calcification and the formation of transparent exopolymer particles (TEP) (Riebesell 2004; Riebesell et al. 2001) are expected to change in an altered physicochemical environment and need further investigation.

The understanding of how nutrient cycling, primary production and species distribution will interact and influence export production in an enviroment of elevated temperatures and changing sea water chemistry is still poor.

1.3. Cyanobacteria

1.3.1. The nitrogen cycles and the role of cyanobacteria

With seven oxidation states and numerous interspecies conversion mechanisms, nitrogen has by far the most complex cycle of all major nutrients (Figure 2).

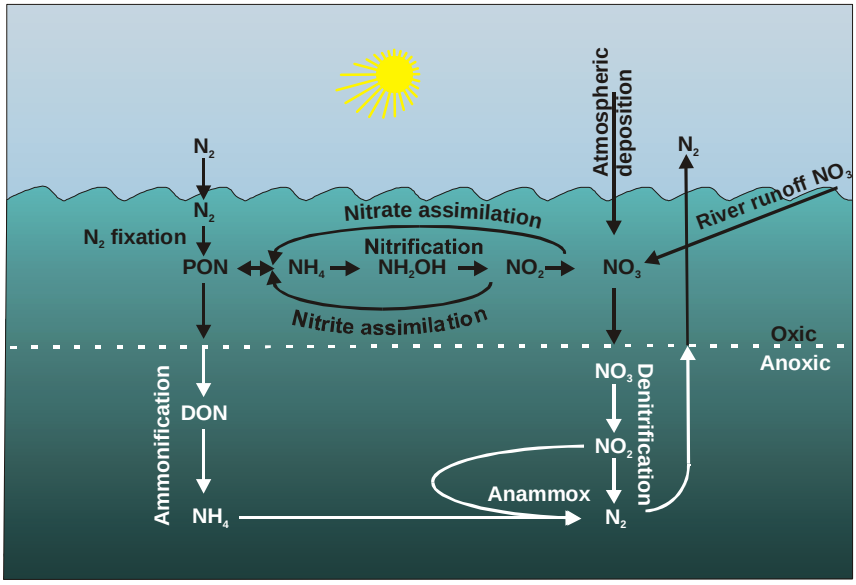

Figure 2: The marine nitrogen cycle modified for the Baltic Sea after Arrigo (2005)

Although diatomic nitrogen (N_2) is almost ubiquitous on earth, as it is the main constituent of the atmosphere, its bio-available forms are usually the limiting factor in biological production (Ryther and Dunstan. 1971; Tyrrell 1999). It is the strong N_2 triple bond that makes the supply of biologically available nitrogen limited to very few natural sources. Whereas anthropogenic nitrogen production (Emsley 2001) and emission of nitrous oxides (NO_x) by fossil fuels combustion are today major sources of bio-available nitrogen (Galloway and Cowling. 2002), bacterial nitrogen fixation is the only natural source of quantitative importance (Figure 2). Planktonic primary production is, at least seasonally, mainly supported by the diazotrophic activity of cyanobacteria. That applies to the oligotrophic open oceans (Galloway et al. 2004; La Roche and Breitbarth. 2005) as well as to the Baltic Sea and freshwater habitats that are subjects to strong anthropogenic nitrogen inputs (Helcom. 2007; Larsson et al. 2001). Diazotrophs themselves and the associated nitrogen input are often limited by the availability of iron and phosphorus (Mills et al. 2004; Paerl et al. 1994).

The different estimates for global oceanic nitrogen fixation by *Trichodesmium* made during the last ten years varied strongly. Recent estimates are more than tenfold higher than those presented in the early 90´s (total range 10-200 Tg yr^{-1})(Jaffe 2000). Other diazotrophic species have been found to contribute to oceanic nitrogen fixation (Zehr et al. 1998). Moreover new methods have been developed showing that even the abundances of species we know are still not well assessed (Davis and McGillicuddy Jr. 2006; Kolber 2006). So estimates are expected to continue to increase.

Denitrification, another microbial activity, converts the combined nitrogen back to atmospheric N_2 (Figure 2). This occurs in anoxic soils, waters and sediments. Despite increasing anthropogenic nitrogen production rates, this process seems to be efficient enough to prevent significant accumulation of combined nitrogen (Galloway et al. 2004). Even though there are substantial uncertainties concerning the rate of biological nitrogen fixation and denitrification, it is argued that the global nitrogen budget is not in a steady state (Falkowski 1997) and turnover rates appear to be fast (~2000 years) (Brandes and Devol. 2002). Hence, small variations in the ratio between nitrogen fixation and denitrification can change global nitrogen budgets and thus control atmospheric CO_2 on a glacial-interglacial time scale (Capone 2001; Deutsch et al. 2007; Mahaffey et al. 2005).

1.3.2. *Nodularia spumigena* and its role in the Baltic Sea

Nodularia spumigena MERTENS is a filamentous heterocystous cyanobacterium which is found in the upper water column positively buoyant by gas vacuoles. The brownish green filaments, sometimes longer than 1 cm, are ~10 µm wide and consist of many cells. A single vegetative cell grows up to 4.5 µm in length (Figure 3).

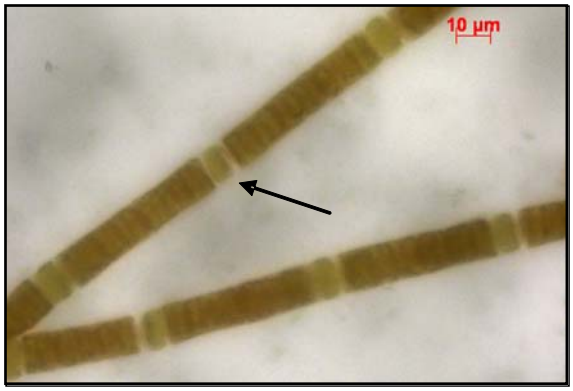

Figure 3: *Nodularia spumigena* filaments with heterocysts (arrow).

There are seven species of genus *Nodularia* in the Nostocales order and the Nostocaceae family currently defined on the basis of morphological characters and ecological requirements

(Komarek et al. 1993). *Nodularia* species are globally distributed in marine and limnic habitats. Only the planktonic species *N. spumigena* and the benthic *N. harveyana* are common in the Baltic Sea (Geidler 1932). *N. spumigena* is a toxic stenohaline species (optimal salinity of ~5-18 (PSU)) (Kononen 1992) which occurs only in saline lakes (Hamilton-Galat and Galat. 1983) and estuaries. Exclusively in the Baltic Sea and in the Peel-Harvey estuary in Australia, *N. spumigena* frequently forms extensive blooms that play a major role in the annual productivity of these regions (Sellner 1997). Estimates of the annual nitrogen fixation of the Baltic cyanobacterial blooms are roughly equal to the total nitrogen input from river runoff and atmospheric deposition. (Larsson et al. 2001; Schneider et al. 2003). But these high external nitrogen inputs (Helcom. 2007) are to be put into perspective of a considerable loss of inorganic nitrogen due to denitrification under the non-periodically occurring anoxic conditions in the Baltic deep basins (Savchuk and Wulff 2001).

The blooms in the Baltic Sea are not solely composed of *N. spumigena*, but also the halotolerant freshwater species *Aphanizomenon flos-aquae* and *Anabaena* sp. as well as picocyanobacteria (mainly *Synechococcus* sp.) are contributing in varying proportions (Stal et al. 2003).

Pigments and $\delta^{15}N$ variations in sediment cores indicate that cyanobacterial blooms have been occurring since the former Ancylus Lake turned into the brackish Littorina Sea about 7000 years ago (Bianchi et al. 2000). However there is a significant increase in bloom frequency and intensity since the 1960`s that can mainly be explained by anthropogenic phosphorus input (Finni et al. 2001).

In phosphorous limiting conditions *Nodularia* forms akinetes, a resting stage that outlasts winter and germinate under conditions when nitrogen is depleted and temperatures reach 16° C (Niemi 1979; Stal et al. 2003). Under calm conditions *Nodularia* accumulates at the surface to big aggregates and even dense scums. The attribute to form surface scums is restricted to blooms of heterocystous cyanobacteria in limnic and brackish habitats (Staal et al. 2003). Within this microenvironment high biomasses of heterotrophic microorganisms are supported (Hoppe 1981). *Nodularia* are degraded mainly in the surface layer due to relatively stable gas vacuoles and the attachment to intact cells (Oliver and Ganf. 2000; Sellner 1997). There are various indications that aggregation is an important part of the competitive strategy of many cyanobacteria (Paerl and Ustach. 1982) but the ecophysiological advantages arising from it are still largely unknown and need further investigation.

1.4. CO_2 effects on phytoplankton physiology

In seawater inorganic carbon is available in surplus and it is common consensus that it does not limit biomass production (Clark and Flynn. 2000), while in fresh and brackish waters the inorganic carbon pool can be substantially reduced due to high photosynthetic activities (Oliver and Ganf. 2000; Thomas and Schneider 1999). The concentration of CO_2, however, represents less than 1% of the inorganic carbon species and does indeed commonly limit photosynthetic rates (Giordano et al. 2005).

Research of the last decade showed that expected changes in seawater chemistry and ocean surface temperatures within climate change will effect ocean primary production in different ways (Riebesell 2004; Sarmiento et al. 2004). Rising CO_2 concentrations as expected for the next century have been shown to facilitate carbon fixation in natural plankton communities (Hein and Sand-Jensen. 1997; Riebesell et al. 2007).

RUBISCO (Ribulose-1,5 bisphosphate carboxylase/oxygenase) is the only enzyme that catalyses CO_2 fixation for carbohydrate synthesis in oxygenic photoautotrophs and has remained nearly unchanged since its evolution under high $[CO_2]$/low $[O_2]$ as it was the case in the early Earth atmosphere (Raven and Johnston. 1991). Even though in eukaryotic organisms the CO_2 affinities of RUBISCO are higher than in cyanobacteria (Raven and Johnston. 1991), it is still substrate limited and shows side reactions with oxygen under current oceanic $[CO_2]$/ $[O_2]$. To guard against this drawback photoautotrophic organisms evolved different active mechanisms to provide elevated $[CO_2]$ at the site of carboxylation (reviewed by Badger et al. (2005) and Badger and Price. (2003)). These carbon concentrating mechanisms (CCM) are composed of diverse transporters that enrich HCO_3^- inside the cell, as well as of carboxysomes, which are bodies that provide a site were the conversion of HCO_3^- to CO_2 by carboanhydrase enzymes is directly associated with RUBISCO (Badger et al. 2005; Giordano et al. 2005).

Being the oldest living oxygenic photoautotrophs, cyanobacteria have experienced dramatic changes in atmospheric $[O_2]$ and $[CO_2]$ and are presently living in a variety of extreme habitats ranging from acidic to alkaline and from hot to cold. They are even successful competitors in environments where inorganic carbon becomes the limiting factor due to high growth densities as prevailing in microbial mats and surface scums (Oliver and Ganf. 2000; Shapiro and Wright 1990). Depending on the conditions in the natural habitats of different cyanobacterial species the set of CCM expressed can strongly differ (Badger et al. 2005). The expression of some CCM is constitutive whereas the expression of other CCM is regulated in response to environmental factors (Beardall and Giordano. 2002; Shibata et al. 2001). Elevated CO_2 concentrations reduce the energy costs for CCM (Fridlyand et al. 1996) and the regeneration of

oxidised carbon acceptors and should thereby facilitate other energy consuming processes (Raven and Johnston. 1991; Riebesell 2004). In cyanobacteria, this could have stimulating effects on growth, nitrogen fixation and nutrient uptake with possible implications on the elemental composition of the formed biomass. An accumulation of carbon relative to nutrients (N, P) could be expected, especially under nutrient limiting conditions (Sterner and Elser. 2002). Enhanced carbon fixation does not necessarily have to be associated with an intracellular carbon accumulation but can also result in increased exudation of dissolved carbohydrates (Engel 2002).

1.5. Related studies and the motivation of this study

Elevated growth rates and nitrogen fixation rates under projected future CO_2 conditions were measured in *Trichodesmium* (Barcelos E Ramos et al. 2007; Hutchings et al. 2007). A combined positive effect of CO_2 enrichment and temperature on growth was observed for *Synechococcus* but not for *Prochlorococcus* under the same conditions (Fu et al. 2007). CO_2 related shifts in elemental ratios were also measured in all of these experiments. But the cyanobacteria in these studies as well as eight different microalgae examined by Burkhardt et al. (1999) reacted differently to rising CO_2. Observed reactions in elemental ratios included increasing, decreasing and constant C/N and C/P ratios. These results imply that the reaction to future CO_2 concentrations will not follow obvious general patterns but may depend on the physiology of single species and perhaps even of single strains.

It is still not known whether different diazotrophic species have distinct physiological responses to rising [CO_2]. And it is an urgent need to examine more representatives of different cyanobacterial groups from different oceanic regions. This study aims to find whether and to what extent the stimulating effects of elevated [CO_2] on growth and nitrogen fixation found in *Trichodesmium* can be generalised for diazotrophic cyanobacteria and be applied to *Nodularia* from the Baltic Sea.

Here carbon and nitrogen fixation of *Nodularia spumigena* is investigated under five different CO_2 concentrations. Simulated conditions correspond to concentrations between glacial and future values projected for 2100. Other environmental conditions are kept constant simulating a pre bloom situation where single filaments are suspended within the surface layer. Under bloom conditions aggregation of filaments typically occurs. This is avoided as microclimate effects in the aggregates might cause significant alteration of CO_2 related physiological effects.

The knowledge obtained gives insights into the eco-physiology of this species and further helps interpretation of data from field observations and mesocosm experiments.

2. Material and methods

2.1. Culture

The culture of non axenic *Nodularia spumigena* was isolated from the Baltic Sea (southern Gothland Sea) in 2000 by Susanne Busch ("Institut für Ostseeforschung Warnemünde" (IOW)). This strain (IOW-2000/1) is free of flagellates.

2.2. Growth media

Batch cultures were grown in artificial seawater based media using modified YBCII (Chen et al. 1996) nutrients without inorganic nitrogen and with reduced phosphate (Table 1). Preliminary tests showed no distinct difference in growth rate between cultures that were grown either in natural or artificial seawater (preliminary test results see annex 2; Figure 20).

Artificial seawater (prepared according to Kester et al. (1967)), was used to reduce bias due to remains of organic nutrients and nitrate. A high value of organic nitrogen (Table 1) was mainly caused by EDTA in the iron solution and partly by vitamins (YBCII nutrients). A salinity of 8 (PSU) was chosen in correspondence with the origin of the culture (Southern Gothland Sea) and because it is the salinity where intensive blooms of *Nodularia* are occurring most often (Kononen 1992). Dissolved inorganic carbon (DIC) concentrations were adjusted to a value similar to the values found in the Baltic Sea (1965 µmol l^{-1}). The media was filtered after preparation by means of a peristaltic pump into sterile one litre Schott Duran bottles (Schott AG, Mainz, Germany) using a Whatman POLYCARB^{TM} 36 AS membrane filter with 0.2 µm pore size (Whatman Maidstone UK). Air bubbles were avoided as far as possible to prevent changes in DIC by outgassing of CO_2. The media for the pre-culture and experiment was prepared from one batch.

The CO_2 manipulation was carried out by adding HCl or NaOH one day before inocculation.

Table 1: Initial concentrations of dissolved nutrients in the growth media

Species	Concentration in µmol l^{-1}
NO_3	0.00
NO_2	0.03
NH_4	0.16
DON	8.05
PO_4	5.44
DOP	0.00

2.3. Experimental setup

Experiments were carried out in a climate chamber at 16° C. This temperature was chosen because *Nodularia* blooms frequently develop in the southern Baltic at this value (Kononen 1992).

The semi continuous batch cultures were illuminated with Phillips TL-D 90 36W-950 fluorescent tubes at an average intensity of 85 µmol photons m^{-2} s^{-1} under a 14/10 h light/dark cycle. To guarantee equal light conditions for all bottles their positions were shifted every day.

In order to allow a correlation of the measured carbonate system parameters of the media with the growth parameters of the culture**,** it is essential to avoid any microclimate effects by keeping the cell filaments in a permanently homogenous suspension. This was assured by a rotating device (Planktongravistat) that rotated the bottles orthogonal to their axis at a constant velocity of 1 rpm (Figure 4 and annex 3).

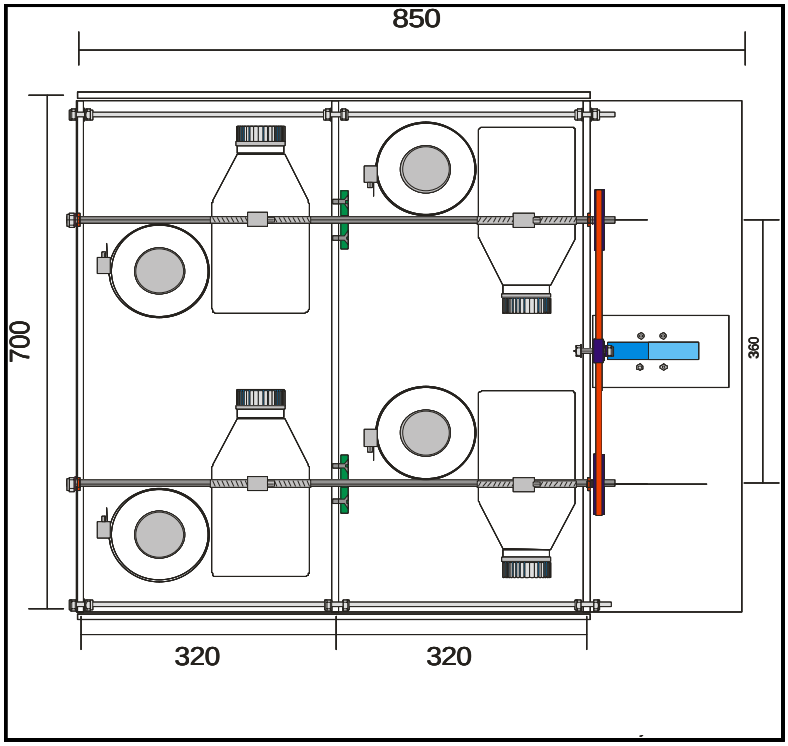

Figure 4: Planktongravistat top view (lengths in mm)

To allow acclimation of the cultures to the five CO_2 treatments of partial pressures ranging from 140 to 630 ppm and corresponding pH ranges from 8.6 to 8.0 (Figure 5) pre-cultures were grown for 13 days, respectively 18 days for the two high CO_2-concentration treatments (equivalent to about seven to eight generations).

For the main experiment the Chl *a* concentrations of pre-cultures were measured in triplicates (~6-12 µg l^{-1}) and diluted to a start value of 1 µg l^{-1} in three replicate bottles per treatment

(Figure 5). The inocculation was done by subtracting the calculated amount of media from the full bottles and replacing it with pre-culture using sterile 50 ml pipettes (Sarstedt, Nümbrecht, Germany). All treatments were sampled after an incubation of seven days.

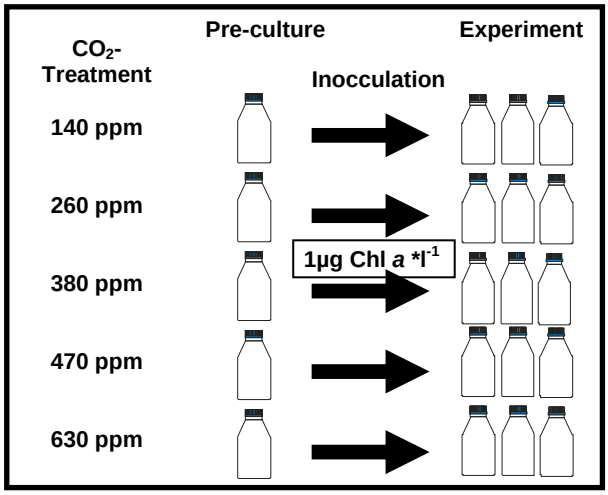

Figure 5: Experimental setup

2.4. The carbonate system

DIC and Total Alkalinity were measured and pCO_2 and pH were calculated with the program CO2SYS version 01.05 by E. Lewis and D. Wallace using the following settings:

1. single input mode
2. constants by Roy et al.
3. pCO_2
4. The K_{SO4} by Dickson
5. pH on the free scale

Both Total Alkalinity and DIC were measured after filtration of the media. The difference to the calculated Alkalinity at the intended CO_2 treatments (Table 2) was determined and adjusted by adding calibrated NaOH (~1 mol l^{-1}) to the three low CO_2 treatments and HCl (~1 mol l^{-1}) to the two high CO_2 treatments.

Table 2: Values of the CO_2 partial pressures and concentrations for the five treatments. Shown are mean values of the three replicates calculated for the point at which half of the DIC consumed during the experiment has been taken up (for single bottle values see annex 1)

Treatment		pCO_2 (ppm)	$[CO_2^*]$ µmol*kg^{-1}	pH
1	Glacial	140	5.9	8.6
2		260	10.9	8.4
3	Present	380	16.0	8.2
4	Future	470	19.8	8.1
5		630	26.5	8.0

2.5. Sampling volumes for particulate parameters

To take a representative sample of randomly distributed particles it is always favourable to choose a sample volume as big as possible (especially if the particles are relatively large like in this case of *Nodularia* filaments several centimetres long), In culture experiments, on the one hand the sampled volume is limited by the amount of culture available and on the other hand by the detection range of the applied analytical methods.

One approach to minimize stochastic variations of biomass in a small sample volume was to shake the culture (violently) before the assay in order to break the filaments into smaller pieces. This strategy had to be abandoned after a preliminary test showed a delay in growth for cyanobacteria that were mechanically stressed in this way (annex 2 Figure 21). In particular, the inocculation and nitrogen fixation samples would be influenced by stress.

This led to the decision to choose sample volumes of more than 50 ml for all particulate parameter measurements and for nitrogen fixation (for sample volumes of individual analyses see 2.6 Analytical methods).

2.6. Analytical methods

2.6.1. Light measurements

A Quantum Scalar Laboratory Irradiance Sensor (QSL-2100, Biospherical Instruments Inc., San Diego, CA, USA) was used to measure the photosynthetic active radiation (400-700 nm) (accuracy ~ 7%).

Light intensities were measured outside the bottles at the height of the axis of the turning device, around which the bottles were rotating. This displays the average light intensities the culture bottles were exposed to.

2.6.2. Dissolved inorganic carbon (DIC)

DIC measurement was carried out after Stoll et al. (2001) in a QUAATRO analyzer (Bran & Lübbe GmbH, Norderstedt, Germany) equipped with a XY-2 sampling unit. The precision and the accuracy that can be reached with this method are ~ 2-3 µmol kg^{-1}.

To avoid contact with the atmosphere**,** DIC samples were taken with a 10 ml syringe and a needle well below the surface and pressed through a 2 µm syringe filter into 5 ml borosilicate vials with screw caps and teflon septa (Roth Rotilabo®, Carl Roth GmbH Karlsruhe, Germany). The vials were filled with the needle positioned on the bottom overflowing about 5 ml and were subsequently closed tightly avoiding air bubbles. The samples were stored in the dark at 4° C. The samples were calibrated against Dickson seawater standard for CO_2 measurement (Marine Physical Laboratory, University of California, Prof. A. G. Dickson).

2.6.3. Total Alkalinity

Duplicates were measured via potentiometric titration (Dickson 1981) with 0.005 M HCl at 20°C in a Metrohm Tiamo automatic titration device (Metrohm GmbH & Co. KG, Filderstadt, Germany) with a precision of ~ 2µmol kg^{-1}.

Samples of ~50 ml were poured into clean and dry PE bottles, poisoned with 10 µl of saturated mercury dichloride solution and stored in the dark at 4° C.

For each measurement a volume of about 15 ml was drawn into a syringe equipped with a 2 µm polycarbonate filter. The mass of water was determined gravimetrically by weighing the syringe before and after pressing the filtrate into the reaction vessel. Between the measurements the syringe and the filter were washed three times with small amounts of sample and the reaction vessel was cleaned with double destilled water and dried with paper towels.

The pH electrode was calibrated with pH buffers 4.0, 7.0 and 9.0 (Merck KgaA, Darmstadt, Germany). Alkalinity measurements with Dickson seawater standard were conduced every day.

2.6.4. Particulate organic carbon (POC) and nitrogen (PON)

Quantification of POC and PON was carried out via an elemental analyzer with a heat conductivity detector EuroVektor EA (EuroVektor S.p.A., Milan, Italy) according to Sharp (1974).

200 ml of sample was filtered at a pressure of ~200 mbar on a combusted (5 h at 500° C) filter (Whatman GF/F 25 mm Ø) which was subsequently stored at -18° C.

Before measurement filters were dried at 60° C for at least 5 h and packed into tin boats.

2.6.5. Particulate phosphorus (POP)

The procedure for POP determination in seawater samples followed Hansen and Koroleff in Grasshoff et al. (1983), but was adapted to the measurement of samples on glass fibre filters.
200 ml of sample were filtered at a pressure of ~200 mbar on combusted (5 h at 500 °C) filters (Whatman GF/F 25 mm Ǿ) and subsequently stored at -18° C.
Biomass was completely oxidised by heating the filters in 50 ml glass bottles (Duran Schott AG, Mainz, Germany) with 35 ml of alkaline peroxodisulphate solution in a pressure cooker.

2.6.6. Chlorophyll *a* (Chl *a*)

Chl *a* concentrations were determined flourometricaly in a Turner flourometer 10-AU (Turner BioSystems, CA, USA) according to Welschmeyer (1994).
Triplicates of 50 ml were filtered at a pressure of ~200 mbar on glass fibre Filters (Whatman GF/F 25 mm Ø) and stored frozen at -18° C in 10 ml PP tubes. Filters were homogenized in a cell homogenizer V2 (Edmund Bühler, Tübingen, Germany) with 5 ml 90% acetone and about 3 ml of a mixture of 2 and 4 mm Ø glass pearls. For extraction another 5 ml of acetone were added and tubes were centrifuged at 5000 rpm. 5 ml of the supernatant was measured.

2.6.7. Dissolved inorganic and organic nutrients

Duplicates of nitrate (NO_3^-), nitrite (NO_2^-) and phosphate (PO_4^{3-}) as well as DON and DOP were measured colorimetric in a spectrophotometer U 2000 (Hitachi-Europe GmBH, Krefeld, Germany) according to Grasshoff et al. (1983) with a precision of ~ ± 0,2 µmol l^{-1}.
For the inorganic nutrient determination 100 ml of each sample was filtered with a syringe filter of 0.8 µm pore size and stored in PE bottles at -18° C.
For a measurement of the organic nutrients, 50 ml of each sample was carefully filtrated using a 60 ml syringe and combusted filters (for 5 h at 500° C) (Whatman GF/F 25 mm Ø). The particle free samples were stored in PE bottles and frozen at -18° C. For decomposition it was mixed with a spattle tip of Oxisolve® (Merck KgaA, Darmstadt, Germany) and heated for 30 min in a pressure cooker. The initial values for inorganic nutrients were subtracted from the values obtained after decomposition.

2.6.8. Nitrogen fixation

Nitrogen fixation was determined by using the acetylene reduction assay with batch incubation technique according to Capone (1993) considering the Bunsen gas solubility coefficient determined for 16 °C by Breitbarth et al. (2004). To convert acetylene reduction into nitrogen fixation a conversion factor of three was used (Capone 1993).

At the beginning of the sampling procedure, right after the DIC samples were taken, duplicate 52 ml samples and one pair of blanks were transferred into cylindrical vials (N20-50 DIN Macherey-Nagel, Düren, Germany) using sterile serological pipettes (Sarstedt, Nümbrecht, Germany). Vials were closed immediately with gas tight caps to prevent changes in the CO_2 concentrations. The vials were put back in the climate chamber at the same light intensity and the culture was kept homogeneous on an orbital shaker (Biometra® Type WT17, Göttingen, Germany).

Two hours before the middle of the photoperiod 2 ml (Vici precision sampling syringe, Baton Rouge, Louisiana, USA) of purified acetylene was injected into the headspace of the vials. They were incubated for four hours over midday. A 2 ml injection is equivalent to 30-35% v/v of the headspace (depending on the precise volume of the vial) and meets the saturation of the nitrogenase according to the previously measured saturation curve (Figure 6).

Measurement was conducted by injecting 300 µl (Gastight® Samplelock 500 µl Syringe, Hamilton, Bonaduz, Switzerland) of the headspace into a gas chromatograph (Shimadzu GC-14B; RT-Alumina™ AL2_O3_Plot Column, Restek GmbH, Bad Homburg, Germany**)** with flame ionization detector. The samples were kept dark at 16 °C in a specially built rack (annex 3) to reduce temperature changes and further acetylene reduction during the acetylene injection and the measurement procedures.

Exact total volume of each vial used was measured gravimetrically by subtracting the weight of the empty vial from the weight of the vial filled to the top with demineralised water at 20° C.

After the experiment the exact volume of added culture was additionally determined by weighing and allowing for the density of seawater at a salinity of 8 (PSU) and a temperature of 16° C.

2.6.8.1. Nitrogenase substrate saturation

Nitrogenase saturation curves were determined for the usually applied 20 ml vials and additionally for 50 ml vials (Figure 6). The proportions of media to headspace in small vials were the same as in large ones. Shape and light properties of both vial types were very similar.

It was expected that resulting saturation curves for both different volumes should have the same run. Large vials should yield a higher precision of measurement because of the more representative sample volume.

Using the large vials the same culture reached nitrogenase saturation at an acetylene concentration of ~25% of the headspace, while in the small vials corresponding values of 50% were needed to reach a maximal metabolic rate. Routinely applied concentrations are 10 - 20 % v/v (Staal et al. 2001). Furthermore the rate was about a quarter lower in the small vials than in

the large ones (Figure 6). The cause of the different results could not be identified but only 50 ml vials were used.

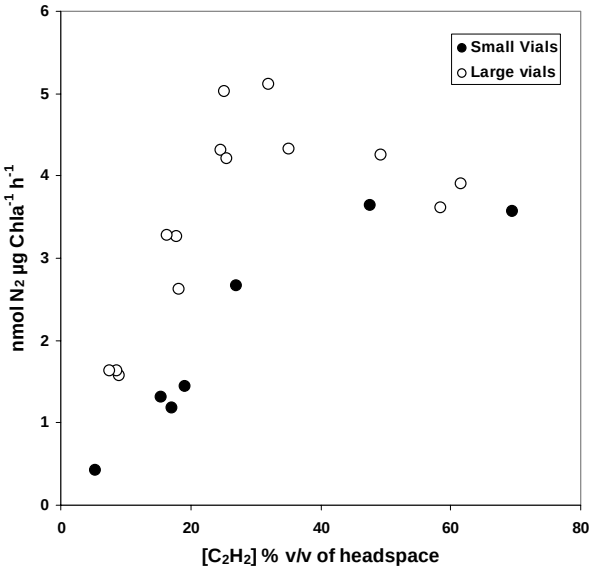

Figure 6: Chlorophyll *a* specific nitrogen fixation at various substrate concentrations for small and large incubation vials.

2.6.9. Cell counts, heterocyst frequency and cell dimensions

Samples were filtered on white cellulose-acetate filters (25 mm Ø 1.2 µm pore size AE95 Schleicher & Schüll, Dassel, Germany) under low vacuum (200 mbar). Photographs were taken with an Observer A1 microscope and an AxioCam MRc (Carl Zeiss, Jena, Germany).

2.6.9.1. Cell dimensions

Samples of 50 ml were filtered and transferred to object carriers and immersed in small amounts of media. Eight spots with many filaments were immediately photographed at 400 times magnification.

Width and length of vegetative cells and heterocysts were measured using the free computer program Image-J (Wayne Rasband, wayne@codon.nih.gov, NIH, Bethesda, MD, USA)

2.6.9.2. Heterocyst frequency

Samples of 50 ml were filtered and transferred to object carrier immersed in small amounts of media and eight spots with many filaments were immediately photographed at 100 times magnification.

The heterocyst frequency was determined by measuring the total length of the filaments with the computer program Image-J, then counting all heterocysts on the picture, subtracting their

summed lengths from the filament length and dividing it by the length of the single vegetative cell. Filaments were analysed until a minimum of 300 heterocysts was counted in each sample. Heterocyst frequency is expressed as vegetative cells per heterocyst.

2.6.9.3. Cell counts

Duplicate samples of 30 ml were filtered and stored dry. 22-28 photos were taken systematically in a transect covering the diameter of the filter and additional 15 photos were taken randomly. Contrast of the photographs was altered by a macro (programmed by Manfried Ditsch) in the computer program Photo Shop version CS3 (Adobe systems, San José, CA, USA) until the cell filaments were entirely black and the background entirely white. (Details of the settings used for the macro are described in annex 4. in German).

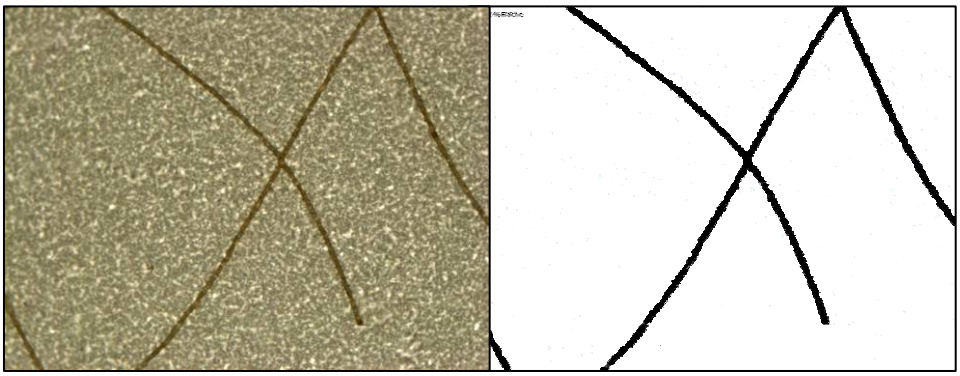

Figure 7: Microscopic picture before (left) and after the macro was applied (right).

Out of a colour histogram a (spreading) value could be achieved that correlated linearly with the surface that was covered by the cells. This spreading value was then correlated with cell counts that were estimated by using the computer program Image-J by measuring the total length of the displayed filaments and dividing it by the length of the single cell. Corrections were made considering the heterocyst frequency and dimensions.

The achieved cell numbers per photo was converted into concentrations per litre sample according to following equation:

$$n/l = \frac{\left(\frac{\sum n_p}{\sum A_p}\right) * A}{V}$$

A_p = Surface area of the single photograph

n_p = Cell number of the single photograph

A = Surface area of the filter containing filaments (filtration funnel d=25mm)

V = Filtered volume of sample

2.7. Statistical methods

For data presentation scatterplots were constructed using the program Statistica 6.0 (StatSoft Inc., Tulsa, USA). Each replicate bottle is represented by one data point. Regression lines represent a Pearson correlation with regression bands depicting the 95% confidence limits and determination coefficient r^2 for the fitted line. The p value is calculated from an f-test testing the null hypothesis that the overall slope is zero and that there is no linear relationship between x and y. Normal distribution of data is assumed.

3. Results

3.1. Growth and cell quota

Growth rates differed significantly among treatments, reaching the highest value of 0.52 d^{-1} at the lowest CO_2 level and the lowest value of 0.33 d^{-1} at high CO_2 levels projected for 2100. This resulted in a total growth rate decrease of 36% (Figure 8). The same trend was observed in four pre-cultures (see annex 2; Figure 22).

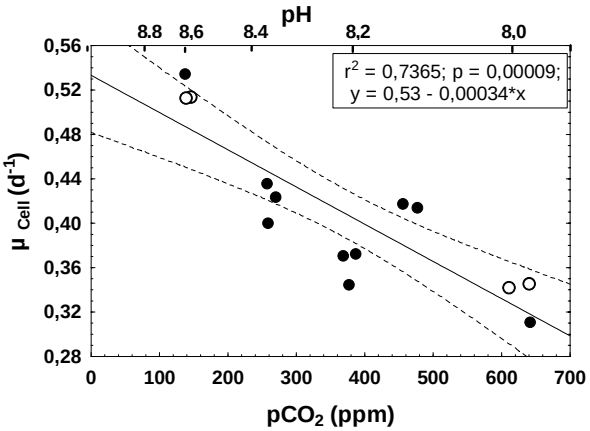

Figure 8: Cellular division rate as a function of CO_2 partial pressure and corresponding pH. Each data point represents one bottle. For the regression line (solid) equation, regression coefficient r^2 and p value are given in the box. The dashed line represents a confident interval of 95%. The marked data points (open circles) are discussed in annex 4

Variations in the quality of the photographs used for automatic cell counting caused variation in estimated cell numbers. Therefore cell number based data showed some outliers and a stronger scattering as non-cellular based data. Anyway, cell numbers are still consistent with results of the chemical analyses and can be used as a biomass indicator for normalisation of these parameters. In the case of the marked data points contrast and colour properties of the photographs differed from the rest of the data set and caused systematic errors. (See annex 4).
While cellular Chlorophyll *a* seemed not to be affected by the CO_2 treatment (Figure 9c) a significant increase in cellular carbon and phosphorus content with rising [CO_2] could be detected (Figure 9a, d). Taking the regression line as a mean, cellular carbon increased from low to high CO_2 treatments by 32% (Figure 9a) and phosphorus increased by 30% (Figure 9d). A similar increase in cellular nitrogen could not be confirmed (Figure 9b) but, excluding outliers (open circles), a trend could be observed.

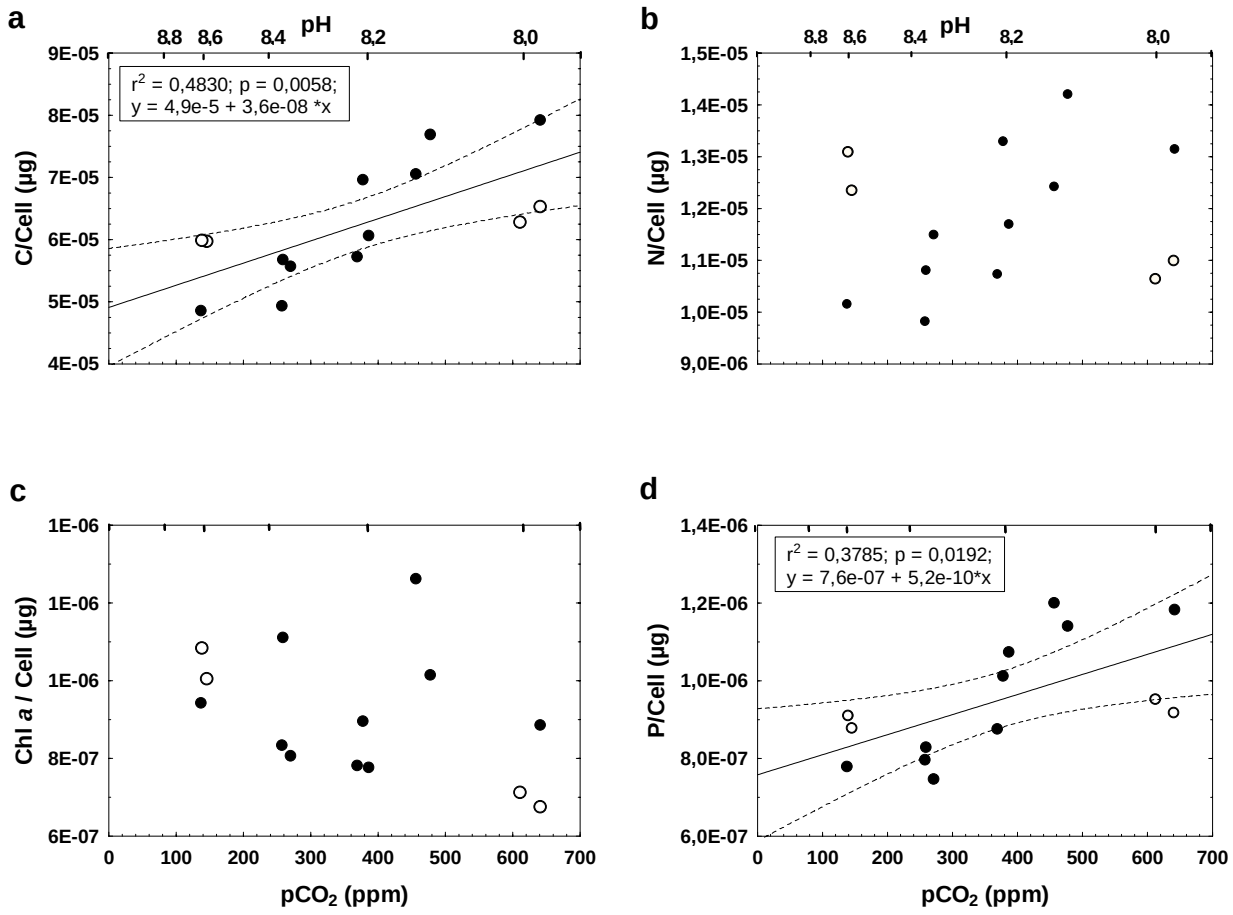

Figure 9: Variations in cell quota of carbon (a), nitrogen (b), Chlorophyll *a* (c) and phosphorus (d) as a function of CO_2 partial pressure and corresponding pH. Each data point represents results from one bottle. For the regression line (solid) equation, regression coefficient r² and p value are given in the box. The dashed line represents a confident interval of 95%. The marked outliers (open circles) are discussed in annex 4

A change in cell dimensions in response to the CO_2 gradient was not observed (Figure 10). Due to the early formation of cross walls (perhaps only pre-prophase band) prior to division, the length of vegetative cells in the cylindrical filament was difficult to measure as the detection of these cross walls strongly depended on the quality of the microscopic preparations and photographs (for cell measurement results see annex1).

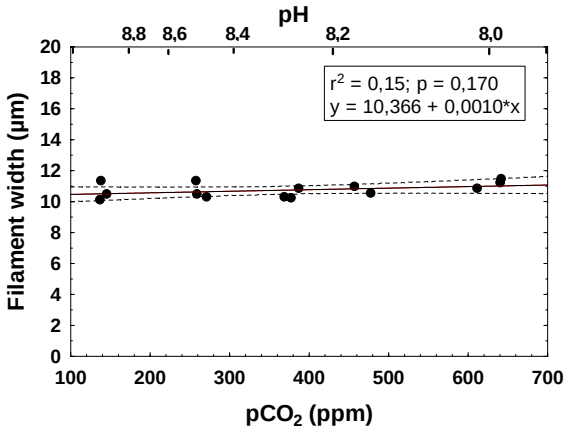

Figure 10: Filament width as a function of CO_2 partial pressure and corresponding pH. Each data point represents results from one bottle. For the regression line (solid) the equation, the regression coefficient r² and p value are given in the box. The dashed line represents a confident interval of 95%.

CO_2 related increase of particulate organic carbon is much more pronounced (65%) when normalised to Chlorophyll *a* than to cell. A value of 55 µmol μg^{-1} was measured for the low [CO_2] treatment while in the high [CO_2] treatment values around 90 µmol μg^{-1} were reached (Figure 11a). Particulate organic nitrogen exhibited the same trend but only about half as strong (31%) with values between 0.84 and 1.1 µmol μg^{-1} (Figure 11b).

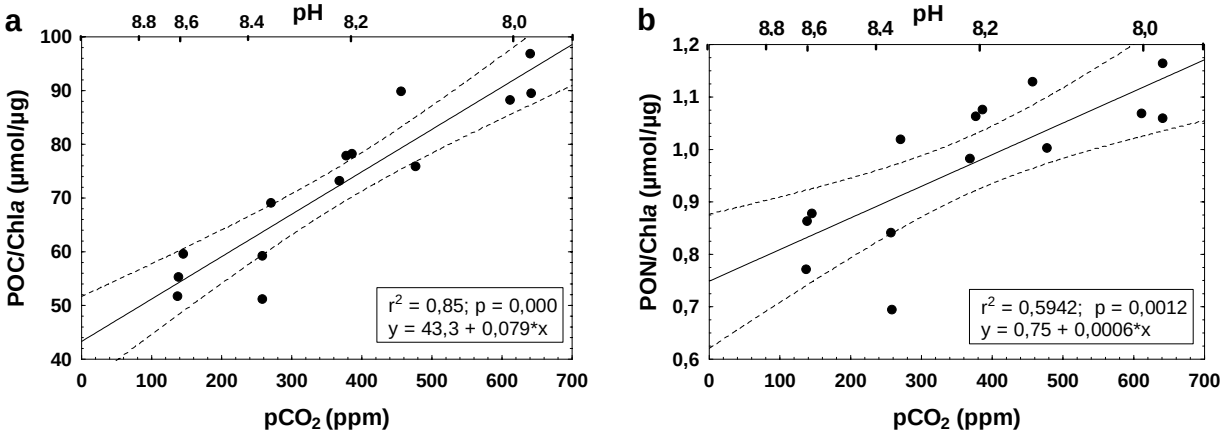

Figure 11: Carbon (a) and nitrogen (b) per Chlorophyll *a* as a function of CO_2 partial pressure and corresponding pH. Each data point represents results from one bottle. For the regression line (solid) the equation, the regression coefficient r² and p value are given in the box. The dashed line represents a confident interval of 95%**.**

3.2. Biomass stoichiometry

Carbon to nitrogen ratios exhibited a highly significant ($p = 0.000$) increase (26%) in response to elevated [CO_2] and lowered pH. At low [CO_2] C/N was about 5.5 and thus below Redfield while a maximum value (7.0) at high [CO_2] was above Redfield (

Figure 12a). In contrast, carbon to phosphorus ratio was not affected by changes in [$CO_{2\ aq}$], remaining constant at about 170, which is 58% above the Redfieldian value (

Figure 12b). As a result of this constancy CO_2 related N/P ratios show a complementary trend to C/N.

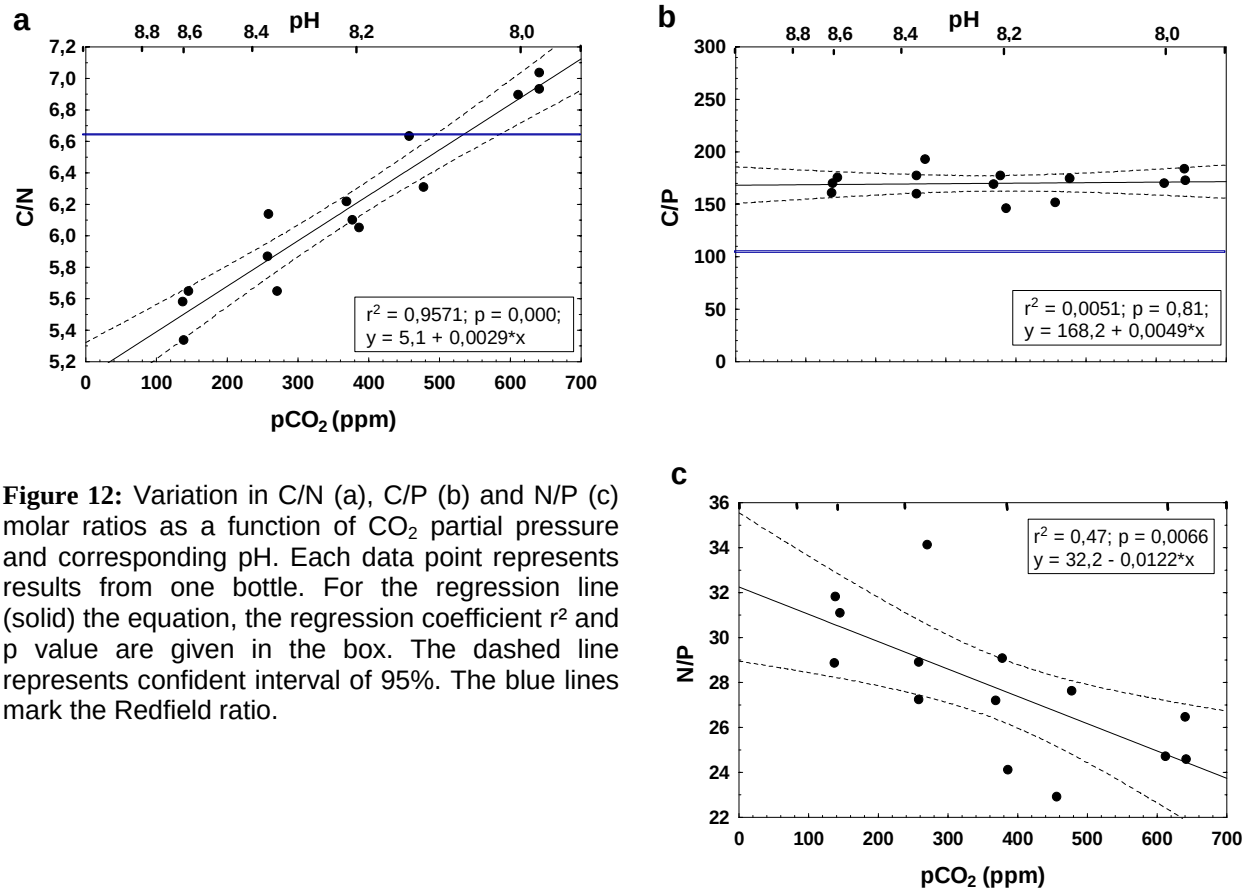

Figure 12: Variation in C/N (a), C/P (b) and N/P (c) molar ratios as a function of CO_2 partial pressure and corresponding pH. Each data point represents results from one bottle. For the regression line (solid) the equation, the regression coefficient r^2 and p value are given in the box. The dashed line represents confident interval of 95%. The blue lines mark the Redfield ratio.

3.3. Nitrogen fixation

Cellular nitrogen fixation rates showed a slight decrease in relation to rising pCO_2 between (Figure 13). However, excluding the outliers it is not significant.

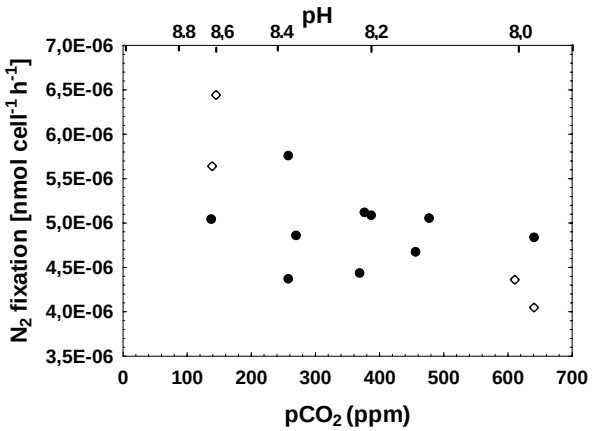

Figure 13: Cellular nitrogen fixation rates as a function of CO_2 partial pressure and corresponding pH. Each data point represents results from one bottle. The marked outliers (open circles) are discussed in annex 4

As can be seen in Figure 14a all treatments exhibit a Chl *a* specific nitrogen fixation rate around 5.5 nmol $h^{-1}\mu g^{-1}$ Chl *a.* An influence due to changes in the carbonate system could not be detected.

In contrast, carbon specific nitrogen fixation rates decreased with rising pCO_2 from 1.29 nmol h^{-1} μmol^{-1} POC at 146 ppm to nearly half of that (0.73) at 642 ppm (Figure 14b). As in this experiment concentrations of particulate phosphorus were always in constant proportion to that of carbon, an analogous trend could be seen when carbon was replaced by POP as a biomass indicator (data not shown).

So if nitrogen fixation in the same plot was normalized to cellular nitrogen contents the decrease was half as steep. Using the regression line as a mean there was is a decline of 25% between the 140 ppm and the 630 ppm treatment (6.7-5.1 nmol h^{-1} μmol^{-1} PON) (Figure 14c).

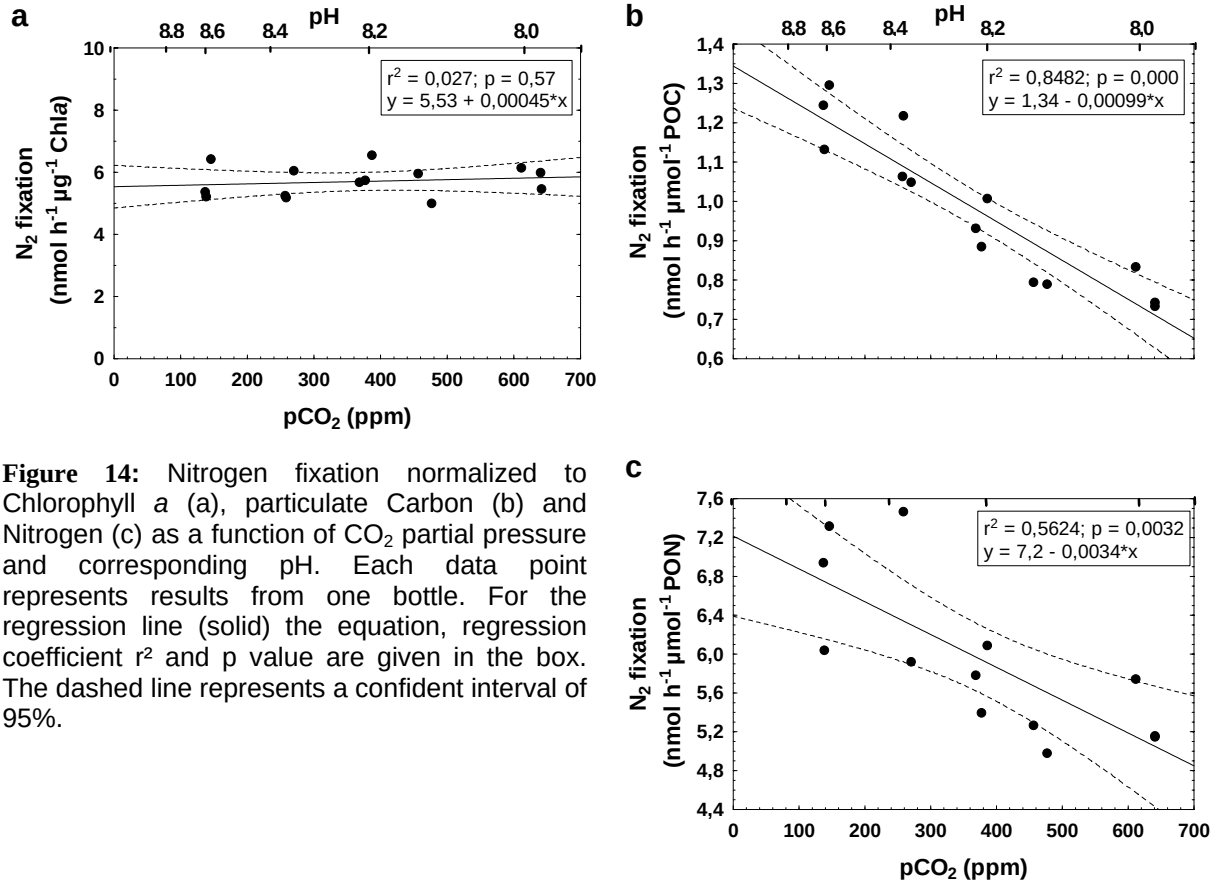

Figure 14: Nitrogen fixation normalized to Chlorophyll *a* (a), particulate Carbon (b) and Nitrogen (c) as a function of CO_2 partial pressure and corresponding pH. Each data point represents results from one bottle. For the regression line (solid) the equation, regression coefficient r² and p value are given in the box. The dashed line represents a confident interval of 95%.

Despite all changes in biomass composition there was no apparent change in heterocyst frequency among the different treatments. On average there were about 11 vegetative cells per heterocyst (Figure 15).

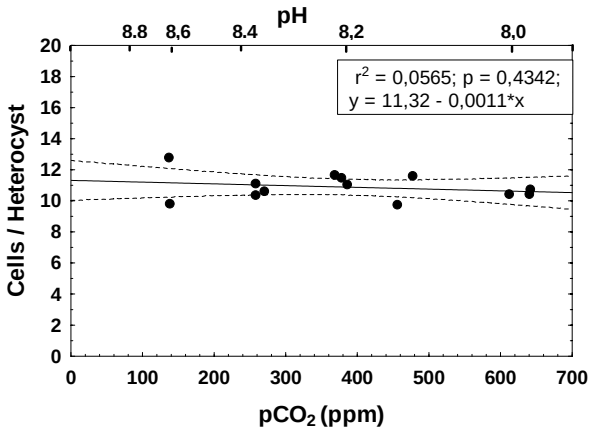

Figure 15: Heterocyst frequency as a function of CO_2 partial pressure and corresponding pH. Each data point represents results from one bottle. For the regression line (solid) the equation, the regression coefficient r² and p value are given in the box. The dashed line represents a confident interval of 95%.

3.4. Uptake and exudation of dissolved substances

Figure 16 shows the uptake of inorganic carbon in relation to the amount of particulate carbon that is formed of it. Obviously there is a general offset that shifts all relations below one. Despite extensive recalculation of all involved datasets back to raw data an error could not be found. Considerations regarding the probability of a systematic error to have occurred rather in the one start measurement than in the two end measurements led to the conclusion that initial DIC concentrations in the media were probably underestimated. At least 25 µmol higher initial [DIC] than by the measurement indicated would shift the ΔDIC/ΔPOC ratios above one.

Nevertheless there is a significant change in the relationship between carbon uptake and storage among the different treatments. High CO_2 grown cultures consumed 39% more DIC per unit POC formed on average than those under low CO_2 conditions.

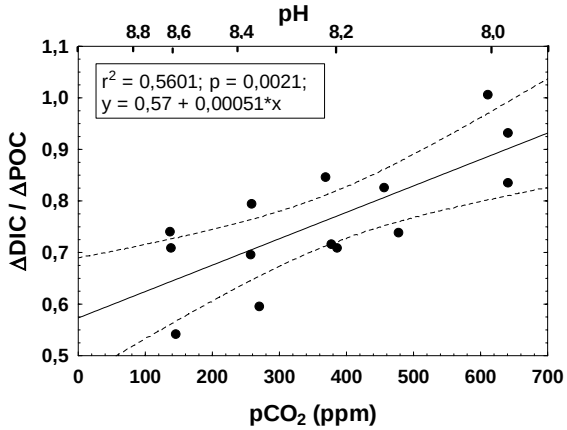

Figure 16: DIC decrease per POC increase (molar ratio) as a function of CO_2 partial pressure and corresponding pH. Each data point represents results from one bottle. For the regression line (solid) the equation, the regression coefficient r^2 and p value are given in the box. The dashed line represents a confident interval of 95%.

The ratio of consumed phosphate per formed particulate phosphorus in relation to rising pCO_2 increases even more than in the case of carbon. A total increase of ~60% between low and high [CO_2] treatments was observed. Taking the regression line as a mean, 2.3 times more DIP is consumed in the low [CO_2] treatment than POP is built up, whereas under high [CO_2] it is 3.7 times more.

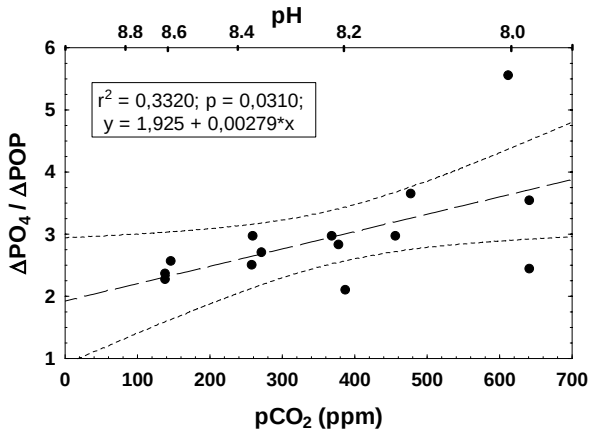

Figure 17: Decrease In dissolved inorganic phosphorus per POP increase (molar ratio) as a function of CO_2 partial pressure and corresponding pH. Each data point represents results from one bottle. For the regression line (solid) the equation, the regression coefficient r^2 and p value are given in the box. The dashed lines represent the 95% confident interval.

The measurement of dissolved organic phosphorus mostly resulted in negative values (phosphate was lost during the digestion procedure) (see annex 1).

Changes in dissolved organic nitrogen were rather small against a large background of organic compounds (EDTA, Biotin, Vitamins). The overall change in that pool was partly positive and partly negative (see annex 1).

4. Discussion

4.1. The growth rate effect

It has been found recently that rising [CO_2] has an effect on growth and carbon fixation in mono specific cultures of eukaryotic (Burkhardt et al. 1999; Riebesell 2004; Yang and Gao 2003) and prokaryotic (Barcelos e Ramos et al. 2007; Fu et al. 2007; Hutchings et al. 2007) marine phytoplankton. In these experiments as well as in studies on natural marine phytoplankton assemblages (Hein and Sand-Jensen. 1997) and in mesocosms (Riebesell et al. 2007) positive influences of increasing [CO_2] on growth and carbon fixation were observed. In contrast, in this study a mono specific culture of *Nodularia spumigena* showed a decrease in division rates in response to CO_2 increase within a similar range. A constant decrease in growth was observed, beginning at the lowest treatment of a CO_2 partial pressure of 140 ppm (pH 8.6), which is even less than the reported values for the last glacial maximum (~180 ppm) (Siegenthaler et al. 2005) over present day values through future values of 630 ppm (pH 8.0). This imposes the assumption that optimal growth of *N. spumigena* is supported by even higher pH and lower [CO_2] than tested - values quite untypical for sea water. Due to the strong buffering effect of the carbonate system, pH of sea water is usually stabilised between 8.1 and 8.3. An ecological approach will be presented that tries to explain the adaptation of *Nodularia* to these high pH values.

For RUBISCO, the enzyme catalysing carbon fixation in photosynthesis, CO_2 is the only inorganic carbon substrate. Ambient CO_2 concentrations in water are mostly not sufficient to reach substrate saturation. Despite the much lower affinity for O_2 oxidation is a problematic side reaction catalysed by RUBISCO under atmospheric O_2 concentrations. In phytoplankton, different carbon concentrating mechanisms (CCM) evolved, ensuring the maintenance of high CO_2 concentrations at the site of carbon fixation. Cyanobacterial CCM are composed of active uptake mechanises that enrich HCO_3^- inside the cells and carboxysomes, bodies where the conversion of HCO_3^- to CO_2 by carboanhydrases is directly associated to RUBISCO (Badger et al. 2005). The performance of CCM in some phytoplankton species is known to be down-regulated under higher ambient CO_2 concentrations due to an increased diffusive uptake of CO_2 or a decreased diffusive loss of CO_2 (Beardall and Giordano. 2002; Shibata et al. 2001). A resulting support of carbon fixation and consequential relief in the cellular energy budget were used to explain stimulating effects of elevated [CO_2] on growth and nitrogen fixation in *Trichodesmium*. This approach can clearly not be used in this study to explain the

impeded growth of *Nodularia*, but also does not have to be necessarily rejected. The accumulation of all major cellular elemental components (C, N, P) indicates that growth was neither limited by carbon fixation nor by energy supply, and both processes could also be enhanced under high [CO_2]. There has to be another mechanism that was affected by the treatment, generally limiting division rates and thus covering the postulated positive effect of high [CO_2] on carbon acquisition. In fact, the accumulation of nutrients in cellular reservoirs and an exudation that can be assumed regarding the $\Delta PO_4/\Delta POP$ and $\Delta DIC/\Delta POC$ ratios, have to be seen as results of the reduced division rate (Kromkamp 1987).

In context of this study, a negative growth rate effect on marine cyanobacteria was most unexpected. But cyanobacteria in terrestrial habitats (i.e. lichens and microbial mats)(Hallingbaeck 1991) and in lakes are known to react in a similar way to acidification as *Nodularia* did in this study (Shapiro and Wright 1990; Whitton and Potts 2000). Acidification caused by anthropogenic atmospheric deposition of strong acids (H_2SO_4, HNO_3) of a similar pH range as applied in this study substantially changed the phytoplankton communities of many lakes. Cyanobacteria were the only phytoplanktonic group that became nearly extinct in these lakes (Findlay 2003). Especially the genus *Nostoc*, a close relative of *Nodularia,* is described by (Mollenhauer et al. 1999) as an "endangered constituent of European inland aquatic biodiversity". (Whitton and Potts 2000) wrote in the introduction of their book on cyanobacterial ecology: "Numerous records for cyanobacteria in freshwater and soils indicate that their diversity and abundance are greatest at high pH values, though the explanation for their particular success under these conditions is still unclear." These statements and the results of the here presented study emphasise that there is an urgent need to investigate pH dependent mechanisms that could be responsible for the observed effects.

4.2. Summarised findings in cell quota

A strong and significant decrease of cellular division rates was detected in response to rising CO_2 concentrations, dominating all measurements (see annex 1). With rising [CO_2] an increase of organic carbon and phosphorus within the cells could be detected while the accumulation of cellular nitrogen was less pronounced. A stronger accumulation of cellular carbon and phosphorus than that of nitrogen under high [CO_2] is supported by a highly significant increase of the elemental C/N ratio. Chlorophyll *a* measurements are much more precise than cell counts. Making use of the C / Chl *a* and the N / Chl *a* ratio, a quantification of the relative increase of carbon to nitrogen quotas is possible, concluding nitrogen accumulated approximately half as strong as carbon.

Although a significant decrease in cellular Chl *a* could not be confirmed, a slightly decreasing trend with rising [CO_2] was observed when comparing the constant ratio of nitrogen fixation per Chl *a* with the decrease of nitrogen fixation per cell (Figure 13). Also the trend in nitrogen fixation per cell is influenced by outliers a slight decrease in cellular Chl *a* seems reasonable. Moreover a negative relationship between Chl *a* / cell and [CO_2] was also observed in pre-cultures (annex 1).

These summarised findings in cell quota are illustrated by (Figure 18)

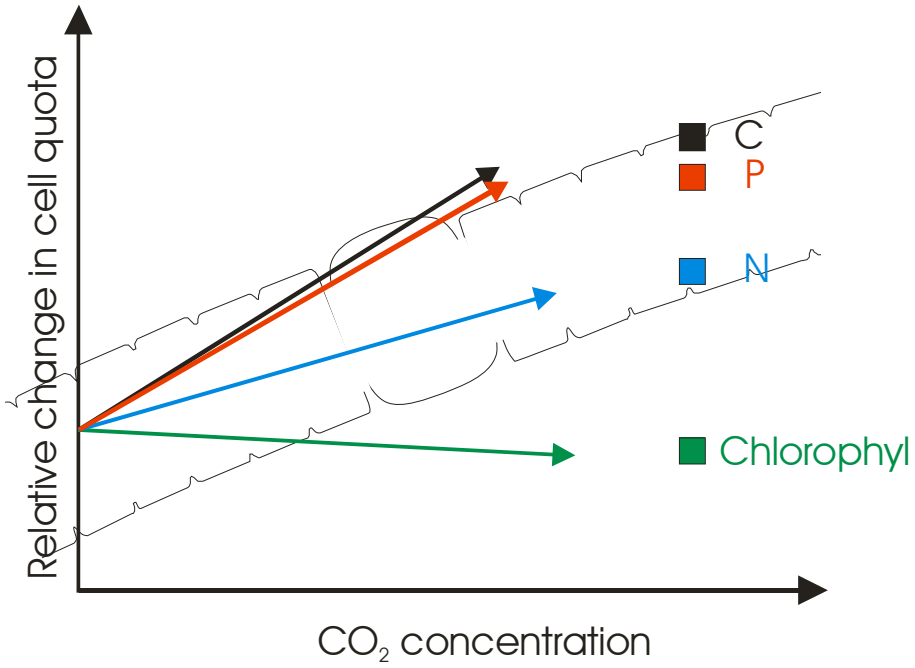

Figure 18: Qualitative comparison of the change in cell quota of carbon (black), phosphorus (red), nitrogen (blue) and chlorophyll (green) over the total range of CO_2 treatments. Slopes of arrows represent the estimated percentile change in the concentration of each constituent in cells.

The Redfieldian concept of a constant elemental composition (106 C : 16 N : 1 P) of average plankton is broadly used as an orientation value in planktology and biogeochemistry when investigating production and nutrient budgets in marine environments (Falkowski 2000). However, the elemental composition of specific phytoplankton groups is known to differ from the Redfield values in respect to the type of structural material they use for cell walls (Sterner and Elser. 2002). Even the stoichiometric composition of a mono specific cell culture can show highly dynamic changes due to its ability to store nutrients in internal pools (Arrigo 2005). A strong tendency to store nutrients is typical for cyanobacteria, especially if they are exposed to high fluctuations in nutrient supply (Allen 1984). Storage mainly occurs in the form of glycogen for carbon, several pigments for nitrogen and polyphosphate for phosphorus.

In this study, the elemental ratio of phosphorous to carbon strongly deviated from Redfield with lower phosphorus contents but did not change in response to the CO_2 treatment. This constancy, and the fact that much higher C/P ratios were observed for *Nodularia spumigena* under P limitation (Degerholm et al. 2006), leads to the assumption that the observed value is just the ratio in which *Nodularia* fixes C and takes up P under replete conditions.

Assuming that limited growth alone resulted in the storage of nutrients that would have otherwise been distributed among daughter cells, a proportional storage of carbon, phosphorus and nitrogen with decreasing growth would have been expected. However, in this experiment, cellular carbon and phosphorus content showed a much stronger increase with rising experimental [CO_2] than cellular nitrogen content. On the one hand this observation could be explained by the observed decrease in cellular nitrogen fixation rates or impeded nitrogen transfer from heterocysts to vegetative cells and on the other hand, by an enhancement of carbon fixation and phosphorus assimilation in vegetative cells due to the CO_2 fertilising effect described above.

4.3. A mechanism that could explain pH sensitivity

While in the non-heteocystic cyanobacterium *Trichodesmium* (Barcelos e Ramos et al. 2007;) nitrogen fixation rates with rising CO_2 levels seemed to benefit of surplus energy from photosynthesis, in this study nitrogen fixation in the heterocystuos *Nodularia* was not enhanced by the treatment. In heterocystous, cyanobacteria nitrogen fixation is spatially separated from the bulk of photosynthetically derived energy. The energy (ATP) and reductive power (NADPH, ferredoxin) for nitrogen fixation in heterocysts is partly derived from cyclic electron transfer in the present photosystem I and partly from the pentose phosphate cycle that is supplied with carbohydrates from vegetative cells (Wolk et al. 1994). Heterocysts are probably not directly affected by [CO_2] as they do not fix CO_2 themselves because they lack photosystem II and RUBISCO (reviewed in Böhme (1998)). However, a pH effect on exchange processes between heterocysts and vegetative cells seems possible. Nitrogen fixed by heterocysts is transferred to vegetative cells by high affinity (active) and low affinity (passive) transport of amino acids (Montesinos et al. 1995). Among others, the acidic amino acid glutamic acid and the basic amino acid arginine play major roles as transporters of fixed nitrogen from heterocysts to the vegetative cells (Böhme 1998). As this exchange occurs mainly by diffusion between the end membranes of two adjacent cells, the amino acids have to pass the external media (Wolk et al. 1994). Due to the ion charge, weak acids can pass transporters only in the protonated form and weak bases can pass only in the deprotonated form. Thus the transport of weak acids and bases shows a high sensitivity to pH

differences among the cell membrane (Decoursey 2003). Based on the findings in pH dependent growth it can be assumed that *Nodularia* is also, concerning its intracellular pH, adapted to live in a basic microenvironment. If the cells cannot adequately adjust the internal pH to more acidic environments, the uptake of basic substances like arginine would be hindered in vegetative cells. The accumulation of metabolites in heterocysts due to an impeded release of acidic compounds like glutamic acid because of an adverse proton gradient among the cell membrane is possible. The potentially hindered release of e.g. glutamic acid could cause an unbalance in the metabolism of heterocysts. This could provide an explanation to the observed decrease in nitrogen fixation rates under low pH. The hypothesis of defective communication between heterocysts and vegetative cells under low pH is supported by the relatively weaker accumulation of particulate organic nitrogen compared to carbon and phosphorous.

The regulation of heterocyst differentiation by the availability of fixed nitrogen has been abundantly demonstrated (see references in Wolk et al. (1994)). The constant heterocyst frequency observed in this study can be seen as an indication of no limitation to growth by the supply of fixed nitrogen to vegetative cells.

4.4. An ecological scenario to explain findings in cell quota

A phenomenon observed for many planktonic, benthic and terrestrial cyanobacteria is the aggregation in clusters and microbial mats. Little is known about whether and how cyanobacteria benefit from this fact. There are only a few studies showing that aggregation can be a purposeful process in cyanobacteria. Kazuko Ohmori et al. (1992) demonstrated spontaneous aggregation of *Spirulina platensis* induced by the application of cyclic adenosine mono phosphate (c-AMP). The same behaviour was observed in *Synechococcus elongatus* in response to a sudden increase in irradiance and was interpreted as a form of light adaptation mechanism (Koblížek et al. 2000).

In the Baltic Sea *Nodularia* is infamous for forming dense toxic surface scums that cause considerable nuisance to the populations of Baltic states every summer. There is ecological evidence that *Nodularia* is specialised in aggregating and that it profits from it. Various studies agree that *Nodularia* dominates the cyanobacterial community under relatively calm weather conditions. When turbid conditions or storms interrupt calm weather picocyanobacteria and other filamentous species that are usually more dispersed in the water column take over (Kononen 1992; Sellner 1997; Stal et al. 2003).

In surface scums, especially in poorly buffered brackish waters like the Baltic Sea (Thomas and Schneider 1999), pH can rise several units and DIC can be significantly lowered due to

high photosynthetic demand for CO_2 (Paerl 2000). According to several authors (Caraco and Miller 1998;Oliver and Ganf. 2000; Shapiro and Wright 1990) cyanobacteria outcompete eukaryotes in carbon acquisition under such high pH and low CO_2 conditions of freshwater blooms. Observations that *Nodularia* showed no CO_2 fertilising effect like *Trichodesmium* could point out that *Nodularia* possess a similar ecological strategy as their freshwater relatives in which the reduction of CCM is not scheduled.

When calm weather leads to an accumulation of *Nodularia* on the surface, high irradiance and associated high photosynthetic activities are likely to promote high nitrogen fixation rates (Paerl et al. 1985). A study of Surosz et al. (2006) showed that *Anabeana flos-aquae,* a relative of *Nodularia* with a similar ecology, reacts to nitrogen starvation with enhanced aggregation due to increased TEP production. In another study, heterocysts of *Anabaena flos-aquae* agglomerated in layers several centimetres thick were shown to exhibit higher nitrogenase activity than that in dispersed filaments, despite high [O_2] caused by photosynthesis in this microenvironment. N : C fixation in filaments outside aggregation was lowest and increased towards the centre (Kangatharalingam et al. 1991). Nitrogen storage is additionally enhanced within surface scums as the microenvironment is enriched with amino acids emitted from heterocysts of neighbouring filaments. In summary, there are many hints supporting the hypothesis that aggregation of heterocystic cyanobacteria is a strategy to improve nitrogen fixation and storage. In contrast, in this study excess consumption of C and P was found in the constantly dispersed *Nodularia* filaments. In nature phosphorus and carbon are in short supply within the surface scum, while small mixing events may provide the possibility for bacteria to store phosphorus and carbon. This ecological scenario (Figure 19) could give a possible explanation for the observed pH preference and the high accumulation of phosphorus and carbon relative to nitrogen in a homogeneously mixed cell culture.

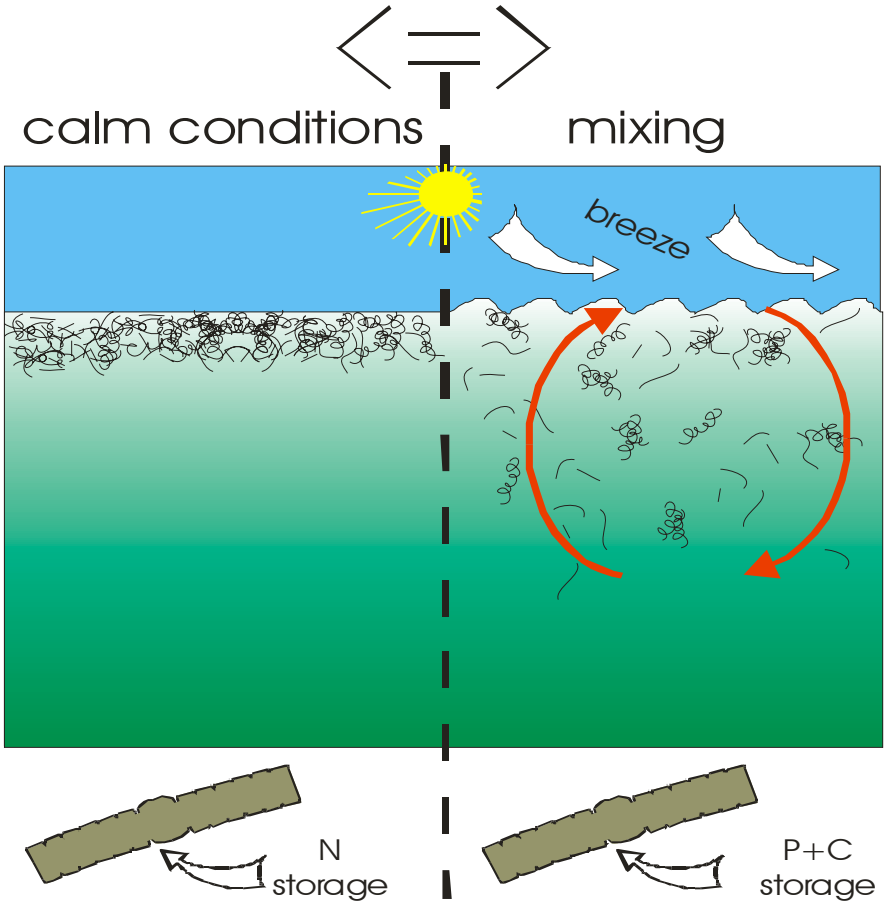

Figure 19: Ecological scenario of alternating surface accumulation (left) and wind induced mixing (right). Schematic filaments and arrows (bottom) illustrate uptake processes that could be favoured under the particular conditions.

4.5. Implications for the Baltic Sea

The physiological response of *Nodularia* in the Baltic Sea to rising atmospheric CO_2 levels and associated acidification has more in common with the responses to similar changes observed in heterocystous cyanobacteria in freshwater blooms than with the salt water examples, like *Trichodesmium* for instance.

In this study it is clearly shown that under pre-bloom-conditions, with single filaments dispersed in the upper water column, growth is highly negatively influenced by acidification. That could lead to a progressive delay in the formation of the characteristic aggregates and thus of the initiation of *Nodularia* blooms with rising atmospheric [CO_2]. As the development of *Nodularia* is delayed, it could be outcompeted by other phytoplankton species that are either less or positively affected by rising [CO_2].

Nodularia, when conglomerated in aggregates or surface scums, probably reacts differently to changes in [CO_2] than the single filaments examined in this study. The question of how carbon and nitrogen fixation within *Nodularia* blooms will develop under the influence of

future elevated CO_2 concentrations cannot be answered by the results presented in this study. Growth of *Nodularia* in a carbon-depleted environment -like a surface scum- is probably enhanced by CO_2 entering from the atmosphere (Oliver and Ganf. 2000; Paerl and Ustach. 1982).

Since cyanobacterial blooms in the Baltic Sea are always composed of different species, it is probable that there will be a gradual change in species composition. The amount of fixed nitrogen during a bloom depends rather on the availability of phosphorous than on the species composition (Arrigo 2005). Therefore, a CO_2 related decrease of the Baltic nitrogen budget cannot be expected. Carbon export is more likely to be enhanced if *N. spumigena* is replaced by different species since it is known that *N. spumigena* decomposes largely in the upper water column, supported by persisting gas vacuoles and living filaments (Hoppe 1981; Sellner 1997). Moreover, the substitution of *Nodularia* by other cyanobacteria could significantly change trophic energy and carbon transfer. *Nodularia spumigena* is the only bloom forming cyanobacterium in the Baltic without metazoan grazers that feed upon it. The energy transfer from *Nodularia* to higher trophic levels via bacteria and micro zooplankton is much less efficient than that from *Anabaena* and *Aphanizomenon* were there is direct grazing.

4.6. What went wrong and how to improve it?

After building the planktongravistat and improving the media there would have been the time to start the first experiment, if it had not been for a single missing piece. A membrane for the auto analyser for DIC measurement was not available and thus the CO_2 treatments calculated could not be checked precisely. Trays to trace the CO_2 treatments by measuring only pH and alkalinity did not lead to satisfactory results. Running an experiment, including all the expensive and time consuming analyses without confirmation of the treatment, did not seem reasonable. Four pre-cultures, each taking about two weeks, were run until DIC measurement was recovered. This time delay was used to test and improve the setup for the final experiment. Concerning the analytical methods, sampling practice and preliminary testing could have considerably improved the achieved results. Due to the limited time given for this diplom thesis, the entire sampling procedure was done only once. With extensive help and instructions of experienced technicians, instructors and colleagues, most of the analyses resulted in feasible data. The measurement of stored DIC samples from pre-cultures, as well as measurements in the experiment, did not always match expectations concerning precision and accuracy. Unaccounted offsets and uncertainties in DIC data, not only in this study, call for a general improvement of sampling and storage in this particular method.

The determination of dissolved organic phosphorous and nitrogen compounds was a complete and unaccountable failure. Since the methodology was correct, possible reasons for the low (and often negative) values might be found for example in adhesive effects of specific compounds of the growth media to the wall of the sampling bottles.

Some extra time would have been needed to substantially improve the cell count method. Due to differences in the camera settings, colour and contrast properties differed among pictures that were taken on different days. As the contrast of the pictures was improved with increasing operating experience, this was not seen as a problem until all data were evaluated. A homogeneous set of photographs could have resulted in much more precise cell count data (see annex 4).

4.7. Perspectives

Over the last years interest in the reaction of marine ecosystems to anthropogenic climate change and resulting consequences for biogeochemical feedback mechanisms influencing oceanic carbon uptake have been steadily growing. The importance of the ecological role of cyanobacteria and the associated input of fixed nitrogen to marine ecosystems has become more and more evident. Experiments with mono-specific cultures showed that there are various effects of rising [CO_2] on carbon and nitrogen fixation in cyanobacteria. Picocyanobacteria and non heterocystic filamentous cyanobacteria seem to react in a totally different way to rising [CO_2] than heterocystic ones. There is clearly a need to further investigate the reactions of more representatives of the different cyanobacterial groups in order to find general patterns in the reactions to elevated [CO_2] at least within the different groups.

The measurement of gradients in pH, [CO_2], [O_2] and nitrogen fixation within dense natural surface scums or artificial aggregations of *N. spumigena* could provide important insights into the ecophysiology of the bloom dynamics of aggregating cyanobacteria.

Furthermore, there are a lot of small puzzle pieces to be joined to prove the hypotheses used to explain the results presented in this study. The "planktongravistat©" as a reliable tool to simulate mixing and stagnation of a water body in order to allow temporal surface aggregation of scum-forming cyanobacteria can be used for incubation of artificial and natural phytoplankton assemblages. Experiments with artificial aggregation could be used to join physiological findings like nutrient storage with ecological findings in bloom dynamics to an ecophysiological strategy as presented above. Different experiments derived from the setup of this study with CO_2 treatments at a constant pH could help separating effects of acidification from direct effects of CO_2 on carbon fixation. The manipulation of temperature as the other

prominent feature of climate change would also be interesting, as well as combinations of temperature and [CO_2].

While there are still uncertainties concerning the cyanobacterial response to rising [CO_2], the even more complex question of the impact of physiological changes on a species level to the functioning of processes like carbon and nitrogen fixation on the ecosystem level arises. The SOPRAN offshore mesocosms experiments planed for summer 2008 will help to further elucidate the response of the natural Baltic phytoplankton community to elevated [CO_2]. The results of this study lead to the assumption that there will be considerable changes on the ecosystem level, since *N. spumigena* plays a substantial role in the summer phytoplankton community of the Baltic Sea.

5. Literature

ALLEN, M. M. 1984. Cyanobacterial cell inclusions. Annual Review of Microbiology **38:** 1-25.

ARCHER, D. 2005. Fate of fossil fuel CO_2 in geologic time. Journal of Geophysical Research **110:** 1-20.

ARRHENIUS, S. 1896. On the influence of carbonic acid in the air upon the temperature of the ground. Philosophical Magazine **41:** 237-276.

ARRIGO, K. R. 2005. Marine microorganisms and global nutrient cycles. Nature **437:** 349-355.

BADGER, M. R., G. D. PRICE, B. M. LONG, and F. J. WOODGER. 2005. The environmental plasticity and ecological genomics of the cyanobacterial CO_2 concentrating mechanism. Journal of Experimental Botany **57:** 259-265.

BADGER, M. R., and G. D. PRICE. 2003. CO_2 concentrating mechanisms in cyanobacteria: molecular components, their diversity and evolution. Journal of Experimental Botany **54:** 609-622.

BARCELOS E RAMOS, J., H. BISWAS, K. G. SCHULZ, J. LAROCHE, and U. RIEBESELL. 2007. Effect of rising atmospheric carbon dioxide on the marine nitrogen fixer *Trichodesmium*. Global Biogeochemical Cycles **21:** 2028 doi:10.1029/2006GB002898.

BEARDALL, J., and M. GIORDANO. 2002. Ecological implications of microalgal and cyanobacterial CO_2 concentrating mechanisms, and their regulation. Functional Plant Biology **29:** 335-347.

BIANCHI, T. S., E. ENGELHAUPT, P. WESTMAN, T. ANDREN, C. ROLFF, and R. ELMGREN. 2000. Cyanobacterial blooms in the Baltic Sea: Natural or human-induced? Limnology and Oceanography **45:** 716-726.

BÖHME, H. 1998. Regulation of nitrogen fixation in heterocyst-forming cyanobacteria. Trends in Plant Science **3:** 346-351.

BRANDES, J. A., and A. H. DEVOL. 2002. A global marine-fixed nitrogen isotopic budget: Implications for Holocene nitrogen cycling. Global Biogeochemical Cycles **16:** 1120 doi: 10.1029/2001GB00185.

BREITBARTH, E., M. M. MILLS, G. FRIEDRICHS, and J. LAROCHE. 2004. The Bunsen gas solubility coefficient of ethylene as a function of temperature and salinity and its importance for nitrogen fixation assays. Limnology and Oceanography Methods **2:** 282-288.

BURKHARDT, S., I. ZONDERVAN, and U. RIEBESELL. 1999. Effect of CO_2 concentration on C: N: P ratio in marine phytoplankton: A species comparison. Limnology and Oceanography **44:** 683-690.

CAPONE, D. G. 1993. Determination of nitrogenase activity in aquatic samples using the acetylene reduction procedure., p. 621-631. *In* P. F. Kemp, B. F. Sherr, E. B. Sherr and J. J. Cole [eds.], Handbook of methods in aquatic microbial ecology. Lewis Publishers.

---. 2001. Marine nitrogen fixation: what's the fuss? Current Opinion in Microbiology **4:** 341-348.

CHEN, Y.-B., J. P. ZEHR, and M. MELLON. 1996. Growth and nitrogen fixation of the diazotrophic filamentous nonheterocystous cyanobacterium *Trichodesmium* sp. IMS 101 in defined media: Evidence for a circadian rhythm. Journal of Phycology **32:** 916-923.

CHRISTOFFERSEN, P., and M. HAMBREY. 2006. Is the Greenland ice sheed in a state of collapse? Geology Today **20:** 98-103.

CLARK, D. R., and K. J. FLYNN. 2000. The relationship between the dissolved inorganic carbon concentration and growth rate in marine phytoplankton. Proceedings of Biological Sciences **267:** 953–959.

DAVIS, C. S., and D. J. MCGILLICUDDY JR. 2006. Transatlantic abundance of the N_2-fixing colonial cyanobacterium *Trichodesmium*. Science **312:** 1517-1520.

DECOURSEY, T. E. 2003. Voltage-gated proton channels and other proton transfer pathways. Physiological Reviews **83:** 475-579.

DEGERHOLM, J., K. GUNDERSEN, B. BERGMANN, and E. SOENDERBAECK. 2006. Phosphorus-limited growth dynamics in two Baltic Sea cyanobacteria *Nodularia* sp. and *Aphanizomenonon* sp. FEMS Microbial Ecolology **58:** 323-332.

DEUTSCH, C., J. L. SARMIENTO, D. M. SIGMAN, N. GRUBER, and J. P. DUNNE. 2007. Spatial cuppeling of nitrogen inputs and losses in the ocean. Nature **445:** 163-167.

DICKSON, A. G. 1981. An exact definition of of total alkalinity and a procedure for the estimation of alkalinity and total inorganic carbon from titration data. Deep-Sea Research **28:** 609-623.

DONEY, S. C. and others. 2007. Impact of anthropogenic atmospheric nitrogen and sulfur deposition on ocean acidification and the inorganic carbon system. Proceedings of the National Academy of Science U S A. **104:** 14580-14585.

EMSLEY, J. 2001. Going one better than nature? Book Review: Enriching the Earth: Fritz Haber, Carl Bosch, and the Transformation of World Food by Vaclav Smil; MIT Press: 2001. Nature **410:** 633-634.

ENGEL, A. 2002. Direct relationship between CO_2 uptake and transparent exopolymer particles production in natural phytoplankton. Journal of Plankton Research **24:** 49-53.

FALKOWSKI, P. G. 1997. Evolution of the nitrogen cycle and its influence on the biological sequestration of CO_2 in the ocean. Nature **387:** 272-275.

---. 2000. Rationalizing elemental ratios in unicellular algae. Journal of Phycology **36:** 3-6.

FEELY, R. A. and others. 2004. Impact of anthropogenic CO_2 on the $CaCO_3$ system in the oceans. Science **305:** 362-366.

FINDLAY, D. L. 2003. Response of phytoplankton communities to acidification and recovery in Killarney Park and the experimental lakes area, Ontario. AMBIO: A Journal of the Human Environment **32:** 190-195.

FINNI, T., K. KONONEN, R. OLSONEN, and K. WALLSTROEM. 2001. The history of cyanobacterial blooms in the Baltic Sea. AMBIO: A Journal of the Human Environment **30:** 172-178.

FORSTER, P., V. RAMASWAMY, and A. OTHERS. 2007. Changes in atmospheric constituents and in radiative forcing., p. 130-236. *In* S. Solomon, D. Qin, M. Manning, Technical support unit, IPCC working group 1 [ed.], Climate Change 2007, The physical science basis. Cambridge University Press.

FRIDLYAND, L., A. KAPLAN, and L. REINHOLD. 1996. Quantitative evaluation of the role of a putative CO_2-scavenging entity in the cyanobacterial CO_2-concentrating mechanism. Biosystems **37:** 229-238.

FRIEDLINGSTEIN, P. and others. 2006. Climate-carbon cycle feedback analysis: Results from the (CMIP)-M-4 model intercomparison. Journal of Climate **19:** 3337-3353.

FU, F. X., M. E. WARNER, Y. H. ZHANG, Y. Y. FENG, and D. A. HUTCHINS. 2007. Effects of increased temperature and CO_2 on photosynthesis, growth, and elemental ratios in marine *Synechococcus* and *Prochlorococcus*. Journal of Phycology **43:** 485-496.

GALLOWAY, J. N., and E. B. COWLING. 2002. Reactive nitrogen and the world: 200 years of change. AMBIO **31:** 64-71.

GALLOWAY, J. N. and others. 2004. Nitrogen cycles: past, present, and future. Biogeochemistry **70:** 153-226.

GEIDLER, L. 1932. Cyanophyceae von Europa., p. 1-1196. *In* Rabenhorst [ed.], Kryptogamenflora. Akademische Verlagsgesellschaft.

GIORDANO, M., J. BEARDALL, and J. A. RAVEN. 2005. CO_2 concentrating mechanisms in algae: Mechanisms, environmental modulation, and evolution. Annual Review of Plant Biology **56:** 99-131.

GRASSHOFF, K., M. EHRHARDT, and K. KREMLING. 1983. Methods of Seawater Analysis., 2 ed. Verlag Chemie.

HALLINGBAECK, T. 1991. Blue-green algae and cyanophilic lichens threatened by air pollution and fertilization. Svensk Botanisk Tidskrift **85:** 87-104.

HAMILTON-GALAT, K., and D. L. GALAT. 1983. Seasonal variation of nutrients, organic carbon, ATP, and microbial standing crops in a vertical profile of Pyramid Lake, Nevada. Hydrobiologia **105:** 1-27.

HEIN, M., and K. SAND-JENSEN. 1997. CO_2 increases oceanic primery produktion. Nature **388:** 526-527.

HELCOM. 2007. Climate change in the Baltic Sea area - HELCOM Thematic Assessment 2007. Baltic Sea Environ. Proc. **111**.

HOPPE, H. G. 1981. Blue-green algae agglomeration in surface water: A microbiotope of high bacterial activity., p. 291-303. *In* G. e. a. Rheinheimer [ed.], Lower Organisms and their Role in the Food Web: Proceedings of the 15th European Marine Biology Symposium, Kiel, Damp 2000.

HUTCHINGS, D. A. and others. 2007. CO_2 control of *Trichodesmium* N_2 fixation, photosynthesis, growth rates, and elemental ratios: Implications for past, present, and future ocean biogeochemistry. Limnology and Oceanography **52:** 1293-1304.

INDERMUEHLE, A. and others. 1999. Holocene carbon-cycle dynamics based on CO_2 traped in ice at Taylor Dome, Antarctica. Nature **398:** 121-126.

IPCC. 2007. http://www.ipcc.ch/graphics/ar4.

ITTEKOT, V. 1996. Particle flux in the ocean. *In* V. Ittekot, P. Schaefer, S. Honjo, and P. J. Depetris. [ed.], SCOPE 96. John Wiley &Sons Ltd.

JAFFE, D. A. 2000. The nitrogen cycle, p. 322-342. *In* M. C. Jacobson, R. J. Charlson, H. Rodhe and G. H. Orians [eds.], Earth System Science. International Geophysics Series. Academic Press limited.

JONES, P. D., and A. MOBERG. 2004. Hemispheric and large-scale surface air temperature variations: An extensive revision and an update to 2001. Journal of Climate **16:** 206-223.

KANGATHARALINGAM, N., W. K. DODDS, J. C. PRISCU, and H. W. PAERL. 1991. Nitrogenase acitivity, photosynthesis, and the degree of heterosyst aggregation in the cyanobacterium *Anabaena flos-aquae*. Journal of Phycology **27:** 680-686.

KASTING, J. F., and J. L. SIEFERT. 2002. Life and the evolution of earth's atmosphere. Science **296:** 1066-1068.

KEELING, C. D., and T. P. WHORF. 2005. Atmospheric CO_2 records from sites in the SIO air sampling network. In Trends: A Compendium of Data on Global Change. US Department of Energy, Oak Ridge, USA Tenn. Carbon Dioxide Information Analysis Center, Oak Ridge National Laboratory.

KESTER, D. R., I. W. DUEDALL, D. N. CONNORS, and R. M. PYTKOWICZ. 1967. Preparation of artificial seawater. Limnology and Oceanography **12:** 176-179.

KOBLÍŽEK, M., J. KOMENDA, J. MASOJÍDEK, and L. PECHAR. 2000. Cell aggregation of the cyanobacterium *Synechococcus elongatus*: Role of the electron transport chain. Journal of Phycology **36:** 662-668.

KOLBER, Z. S. 2006. Getting a better picture of the ocean's nitrogen budget. Science **312:** 1479 - 1480.

KOMAREK, J., M. HUEBEL, H. HUEBEL, and J. SMARDA. 1993. The Nodularia studies 2. Taxonomie., p. 1-21, Archiv fuer Hydrobiologie. Schweizerbart`sche Verlagsbuchhandlung.

KONONEN, K. 1992. Dynamics of the toxic cyanobacterial blooms in the Baltic Sea. Finnish Marine Research **261:** 3-36.

KROMKAMP, J. 1987. Formation and functional significance of storage products in cyanobacteria. New Zealand Journal of Marine and Freshwater Research **21:** 457-465.

LA ROCHE, J., and E. BREITBARTH. 2005. Importance of the diazotrophs as a source of new nitrogen in the ocean. Journal of Sea Research **53:** 67-91.

LARSSON, U., S. HAJDU, J. WALVE, and R. ELMGREN. 2001. Baltic Sea nitrogen fixation estimated from the summer increase in upper mixed layer total nitrogen. Limnology and Oceanography **46:** 811-820.

LAWS, E. A., P. G. FALKOWSKY, W. O. SMITH JR., H. DUCKLOW, and J. J. MACCARTHY. 2000. Temperature effects on export produktion in the open ocean. Global Biogeochemical Cycles **14:** 1231-1246.

MAHAFFEY, C., A. F. MICHAELS, and D. G. CAPONE. 2005. The conundrum of marine N_2 fixation. American Journal of Science **305:** 546-595.

MEEHL, G. A. and others. 2007. Global climate projections., p. 748-845. *In* S. Solomon, D. Qin, M. Manning, Technical support unit, IPCC working group 1 [ed.], Climate Change 2007, The physical science basis. Cambridge University Press.

MILLS, M. M., C. RIDAME, M. DAVEY, J. L. ROCHE, and R. J. GEIDER. 2004. Iron and phosphorus co-limit nitrogen fixation in the eastern tropical North Atlantic. Nature **429:** 292-294.

MOLLENHAUER, R. B. D., and E.-A. LINDSTROM. 1999. Macroscopic cyanobacteria of the genus *Nostoc*: a neglected and endangered constituent of European inland aquatic biodiversity. European Journal of Phycology **34:** 349-360.

MONTESINOS, M. L., A. HERRERO, and E. FLORES. 1995. Amino acid transport systems required for diazotrophic growth in the cyanobacterium *Anabaena* sp. strain PCC 7120. Journal of Bacteriology **177:** 3150-3157.

NIEMI, A. 1979. Blue-green algal blooms and N: P ratio in the Baltic. Acta Botanica Fennica **110:** 57-61.

OHMORI, K., M. HIROSE, and M. OHMORI. 1992. Function of cAMP as a mat-forming factor in the cyanobacterium *Spirulina platensis.* Plant and Cell Physiology **33:** 21-25.

OLIVER, R. L., and G. G. GANF. 2000. Freshwater blooms., p. 149-194. *In* B. A. Whitton and M. Potts [eds.], The Ecologie of Cyanobacteria. Kluwer Academic Publishers.

OSCHLIES, A. 2001. Model-derived estimates of new production: New results point towards lower values. Deep Sea Research Part II: Topical Studies in Oceanography **48:** 2173-2197.

OTTO-BLIESNER, B. L., J. S. MARSHALL, J. T. OVERPECK, G. H. MILLER, A. HU, and CAPE LAST INTERGLACIAL PROJECT MEMBERS. 2006. Simulating Arctic climate warmth and ice field retreat in the last interglaciation. Science **311:** 1751-1753.

PAERL, H. W. 2000. Marine plankton. *In* W. B. Whitton and M. Potts [eds.], The Ecologie of Cyanobacteria. Kluwer Academic Publishers.

PAERL, H. W., P. T. BLAND, N. D. BOWLES, and M. E. HAIBACH. 1985. Adaptation to high-intensity, low-wavelength light among surface blooms of the cyanobacterium *Microcystis aeruginosa.* Applied Environmental Microbiology **49:** 1046-1052.

PAERL, H. W., L. E. PRUFERT-BEBOUT, and C. GUO. 1994. Iron-stimulated N_2 fixation and growth in natural and cultured populations of the planktonic marine cyanobacteria *Trichodesmium* sp. Applied Environmental Microbiology **60:** 1044-1047.

PAERL, H. W., and F. USTACH. 1982. Blue-green alcal scums: An explanation for their occurrence during freshwater blooms. Limnology and Oceanograhy **27:** 212-217.

PETIT, J. R. and others. 1999. Climate and atmospheric history of the past 420,000 years from the Vostok ice core, Antarctica. Nature **399:** 429-436.

RAVEN, J. A., and A. M. JOHNSTON. 1991. Mechanisms of inorganic-carbon in marine phytoplankton and their implications for the use of other resources. Limnology and Oceanography **36:** 1701-1714.

RIEBESELL, U. 2004. Effects of CO_2 enrichment on marine phytoplankton. Journal of Oceanography **60:** 719-729.

RIEBESELL, U. and others. 2007. Enhanced biological carbon consumption in a high CO_2 ocean. Nature **450:** 545-548.

RIEBESELL, U., I. ZONDERVAN, B. ROST, and R. E. ZEEBE. 2001. Effects on increasing athmospheric CO_2 on phytoplankton communitys and the biological carbon pump. Global Change Newsletter **47:** 12-15.

RYTHER, J. H., and W. M. DUNSTAN. 1971. Nitrogen, phosphorus, and eutrophication in coastal marine enviroment. Science **171:** 1008-1012.

SABINE, C. L. and others. 2004. The oceanic sink for anthropogenic CO_2. Science **305:** 367-371.

SARMIENTO, J. L. and others. 2004. Response of ocean ecosystems to climate warming. Global Biogeochemical Cycles **18:** 1-23.

SAVCHUK, O., and F. WULFF. 2001. A model of the biogeochemical cycles of nitrogen and phosphorus in the Baltic. *In* P. Larsson [ed.], A systems analysis of the Baltic Sea. *Ecological Studies: analysis and synthesis*. Springer.

SCHNEIDER, B., G. NAUSCH, K. NAGEL, and N. WASMUND. 2003. The surface water CO_2 budget for the Baltic Proper: A new way to determine nitrogen fixation. Journal of Marine Systems **42:** 53-64.

SELLNER, K. G. 1997. Physiology, ecology, and toxic properties of marine cyanobacteria blooms Part 2: The ecology and oceanography of harmful algal blooms. Limnology and Oceanography **42:** 1089-1104.

SHAPIRO, J., and D. I. WRIGHT. 1990. Current beliefs regarding dominance by blue- greens: The case for the importance of CO_2 and pH. Verhandlungen IVTLAP **24:** 38-54.

SHARP, J. H. 1974. Improved analysis for "particulate" organic carbon and nitrogen from seawater. Limnology and Oceanography **19:** 984-989.

SHIBATA, M. and others. 2001. Distinct constitutive and low-CO_2-induced CO_2 uptake systems in cyanobacteria: Genes involved and their phylogenetic relationship with

homologous genes in other organisms. Proceedings National Academy of Science U S A **98:** 11789-11794.

SIEGENTHALER, U. and others. 2005. Stable carbon cycle-climate relationship during the late Pleistocene. Science **310:** 1313 - 1317.

STAAL, M., S. T. LINTEL-HEKKERT, F. HARREN, and L. STAL. 2001. Nitrogenase activity in cyanobacteria measured by the acetylene reduction assay: a comparison between batch incubation and on-line monitoring. Environmental Microbiology **3:** 343–351.

STAAL, M., F. J. R. MEYSMAN, and L. J. STAL. 2003. Temperature excludes N_2-fixing heterocystous cyanobacteria in the tropical oceans. Nature **425:** 504-507.

STAL, L. J. and others. 2003. Baltic Sea cyanobacteria. An investigation of the structure and dynamics of water blooms of cyanobacteria in the Baltic Sea-responses to a changing environment. Continental Shelf Research **23:** 1695-1714.

STERNER, R. W., and J. J. ELSER. 2002. Ecological stoichiometry. Princeton University Press.

STOLL, M. H. C., K. BAKKER, G. H. NOBBE, and R. R. HAESE. 2001. Continous-flow analysis of dissolved inorganic carbon in sea water. Analytical Chemistry **73:** 4111-4116.

SUROSZ, W., K. A. PALINSKA, and A. RUTKOWSKA. 2006. Produktion of transparent exopolymer particles (TEP) in the nitrogen fixing cyanobacterium *Anabaena flos-aque*. Oceanologia **48:** 385-394.

TAKAHASHI, T. 2004. The fate of industrial carbon dioxide. Science **305:** 352-353.

THOMAS, H., and B. SCHNEIDER. 1999. The seasonal cycle of carbon dioxide in Baltic Sea surface water. Journal of Marine Systems **22:** 53-67.

TYRRELL, T. 1999. The relative influences of nitrogen and phosphorus on oceanic primary production. Nature **400:** 525-531.

WELSCHMEYER, N. A. 1994. Fluorometric analysis of chlorophyll a in in the presence of chlorophyll b and pheopigments. Limnology and Oceanograhy **29:** 1985-1992.

WHITTON, B. A., and M. POTTS. 2000. Introduction to the Cyanobacteria, p. 1-11. *In* B. A. Whitton and M. Potts [eds.], The Ecologie of Cyanobacteria. Kluwer Academic Publishers.

WOLK, C. P., A. ERNST, and J.ELHAI. 1994. Heterocyst metabolism and development, p. 769-823. *In* D. A. Bryant [ed.], The Mollecular Biologie of Cyanobacteria. Kluwer Academic Publishers.

YANG, Y., and K. GAO. 2003. Effects of CO_2 concentrations on the frshwater micoalgae *Clamydomonas reinhardii, Chlorella pyrenoidosa* and *Scenedesmus obliquus* (Chlorophyta). Journal of Applied Phycologie **00:** 1-11.

ZEHR, J. P., M. T. MELLON, and S. ZANI. 1998. New nitrogen-fixing microorganisms detected in oligotrophic oceans by amplification of nitrogenase (nifH) genes. Applied Environmental Microbiologie **64:** 3444-3450.

6. Annex

6.1. Raw data

Table 3: Parameters of the carbonate system. Single bottle values for the five treatments calculated for the point at which half of the DIC consumed during the experiment has been taken up (1-15) and values for pre-cultures (pre1-5) at the time of inoculation.

Replicate	pCO_2 (ppm)	pH	Alkalinity (µmol kg^{-1})	DIC Start (µmol kg^{-1})	DIC End (µmol kg^{-1})
1	146	8.59	2188	1967	1926
2	138	8.61	2193	1967	1914
3	139	8.61	2191	1967	1913
4	258	8.36	2090	1967	1923
5	259	8.36	2091	1967	1926
6	271	8.34	2088	1967	1931
7	378	8.21	2051	1967	1939
8	369	8.22	2051	1967	1934
9	387	8.19	2047	1967	1937
11	457	8.12	2022	1967	1925
12	478	8.10	2019	1967	1927
13	642	7.98	1985	1967	1917
14	612	8.00	1987	1967	1914
15	641	7.98	1986	1967	1919
pre 1	191	8.48	2150	1967	1946
pre 2	300	8.30	2083	1967	1947
pre 3	424	8.16	2042	1967	1946
pre 4	487	8.10	2020	1967	1933
pre 5	576	8.02	1985	1967	1900

Table 4: Single measurements of particulate organic nutrients in the different replicate bottles.

Replicate	POC µmol l^{-1}	PON µmol l^{-1}	POP µmol l^{-1}
1	81.6	14.4	0.47
2	77.0	13.8	0.48
3	81.2	15.2	0.48
4	62.7	10.7	0.39
5	56.3	9.2	0.32
6	65.0	11.5	0.34
7	44.8	7.3	0.25
8	44.4	7.1	0.26
9	47.5	7.9	0.33
11	57.5	8.7	0.38
12	61.0	9.7	0.35
13	59.2	8.4	0.34
14	58.3	8.5	0.34
15	62.2	9.0	0.34

Table 5: Single measurements of acetylene reduction in the different CO_2 treatments.

Treatment	Replicate	C_2H_2 reduktion (nmol l^{-1} h^{-1})
140 ppm	1a	100.5
	1b	110.7
	2a	94.4
	2b	97.2
	3a	90.0
	3b	93.7
260 ppm	4a	72.4
	4b	61.0
	5a	71.5
	5b	65.3
	6a	64.6
	6b	71.6
380 ppm	7a	39.3
	7b	39.9
	8a	37.4
	8b	45.1
	9a	45.7
	9b	49.9
470 ppm	11a	44.2
	11b	47.2
	12a	50.6
	12b	45.7
630 ppm	13a	44.3
	13b	42.5
	14a	50.2
	14b	46.8
	15a	43.6
	15b	48.8

Table 6: Average of cell measurements used for calculation of cell counts with standard deviation and sample size.

Parameter		L (µm)	Standard Deviation	Cells measured
Heterocyst	**Length**	9.8	1.5	111
Vegetative Cell	**Length**	3.83	0.28	601
	Width	10.7	0.54	**180**

Table 7: Cell numbers. heterocyst frequency and filament width at the end of the experiment (1-15) and cell numbers at the beginning of the experiment (derived from pre-culture cell numbers and inocculation volumes (Start 1-5).

Replicate	Cells l^{-1}	µm Heterocyst^{-1}	Filament Width (µm)
1	1.62E+07	51.5	10.5
2	1.90E+07	58.6	10.1
3	1.63E+07	47.4	11.3
4	1.53E+07	49.4	11.4
5	1.19E+07	52.2	10.5
6	1.40E+07	50.3	10.3
7	7.74E+06	53.7	10.2
8	9.31E+06	54.3	10.3
9	9.40E+06	52.1	10.8
11	9.78E+06	47.0	10.9
12	9.53E+06	54.2	10.5
13	8.97E+06	50.8	11.5
14	1.11E+07	49.8	10.9
15	1.14E+07	49.8	11.2
Start 1	4.52E+05		
Start 2	7.26E+05		
Start 3	6.96E+05		
Start 4	5.28E+05		
Start 5	1.02E+06		

Table 8: Change in the concentrations of the different dissolved nutrients over the experimental time course (7 days).

Replicate	ΔDOP	ΔDON	ΔPO_4	ΔNO_2	ΔNO_3	ΔNH_4
1	-0.38	-1.31	-1.20	0.01	0.19	-0.17
2	0.00	2.12	-1.13	0.02	0.46	-0.15
3	-0.10	1.46	-1.08	0.02	0.42	-0.18
4	0.07	1.97	-0.98	0.01	0.64	-0.16
5	-0.56	0.58	-0.94	0.02	0.16	-0.15
6	-0.80	-0.07	-0.91	0.01	-0.05	-0.15
7	-0.90	-1.65	-0.72	0.02	-0.03	-0.11
8	0.03	1.41	-0.78	0.02	0.07	-0.01
9	-0.05	1.39	-0.69	0.02	-0.01	-0.12
11	0.29	1.98	-1.13	0.00	-0.01	
12	0.47	0.78	-1.28	0.00	0.09	
13	0.43	0.41	-1.21	0.02	0.08	
14	0.84	0.32	-1.90	0.00	-0.15	
15	-1.13	-1.41	-0.83	0.00	-0.09	

Table 9: Single measurements of Chlorophyll *a* in Replicate Bottles of the different CO_2 treatments.

Treatment	Replicate	Chlorophyll a (µmol l^{-1})
140 ppm	1a	19.0
	1b	15.3
	1c	15.1
	2a	18.2
	2b	16.7
	2c	18.7
	3a	18.1
	3b	18.2
	3c	16.7
260 ppm	4a	13.6
	4b	12.3
	4c	12.2
	5a	13.5
	5b	14.4
	5c	11.8
	6a	11.2
	6b	11.6
	6c	11.1
380 ppm	7a	7.5
	7b	7.3
	7c	5.9
	8a	6.8
	8b	7.5
	8c	7.6
	9a	7.8
	9b	7.0
	9c	7.1
470 ppm	11a	7.6
	11b	6.7
	11c	8.8
	12a	9.0
	12b	10.0
	12c	9.9
630 ppm	13a	8.2
	13b	8.5
	13c	7.1
	14a	7.8
	14b	7.8
	14c	8.2
	15a	8.0
	15b	8.3
	15c	6.9

6.2. Preliminary Tests

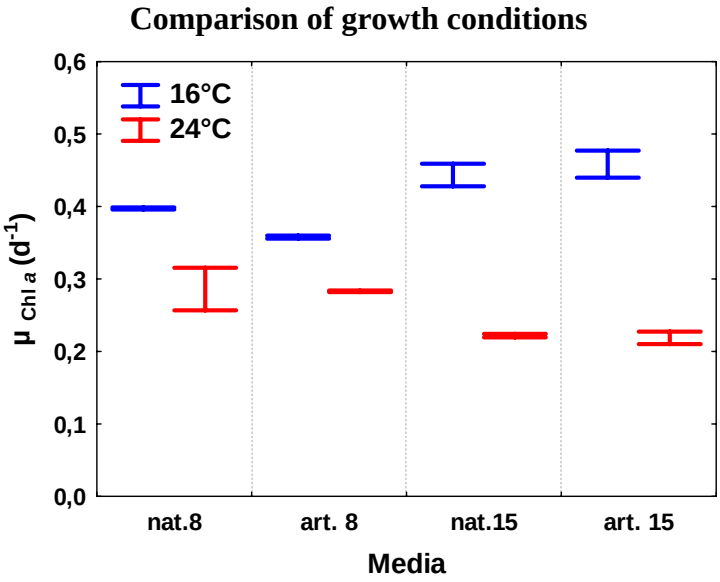

Figure 20: Chlorophyll *a* derived growth rates for *Nodularia* grown on artificial (art) and natural (nat) sea water with salinities of 8 and 15 (PSU). Two different Temperatures were tested 24°C (red) 16°C (blue). Whiskers represent two replicate bottle values.

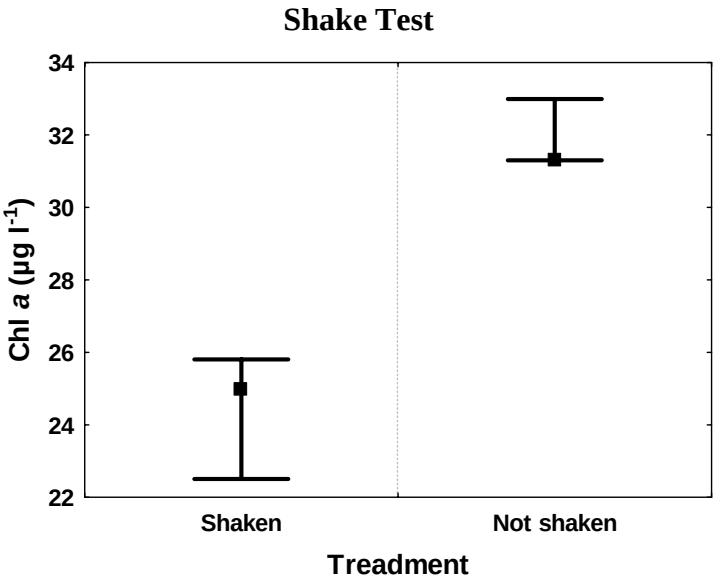

Figure 21: Chlorophyll *a* concentrations in *Nodularia* cultures after fife days of growth. Inocculation was conducted adding the same amount of the same pre-culture with filaments broken to ~5mm pieces (Shaken) and intact filaments (Not shaken). Whiskers and datapoints represent three replicate bottle values (min., max. and median).

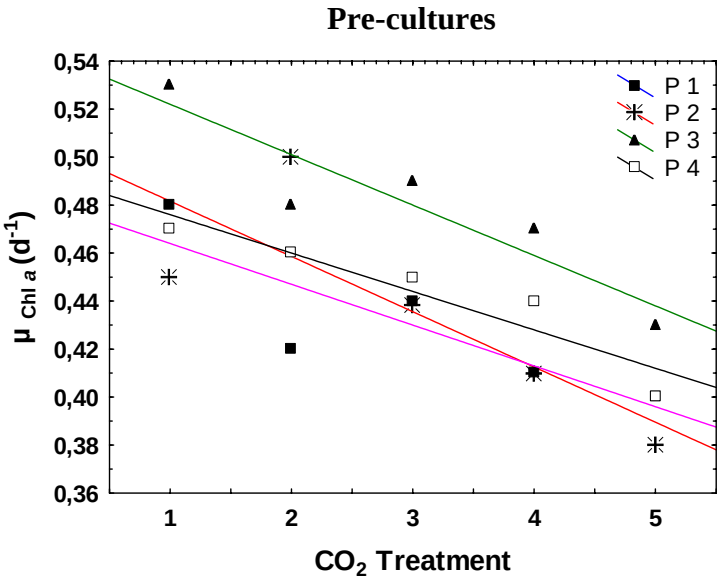

Figure 22: Chlorophyll *a* derived growth rates for four pre-cultures grown under low [CO_2] (treatment one) to high [CO_2] (treatment five). Experimental setup is equivalent to the setup of the main experiment (material and methods). CO_2 manipulation was conduced like in the experiment but measurements of discreet values are not available because of technical problems with the DIC analysis.

6.3. Construction of the planktongravistat

A gentle way of keeping a culture suspended

Cell cultures need finely-tuned and controlled stable conditions to grow. Stagnation of media in culture bottles and aggregation of cells has to be avoided to prevent the build up of a microclimate of nutrient depletion, oxygen or CO_2 depletion or accumulated toxic by-products. Currently there are a number of devices on the market that shake, rattle, role or stir the cell cultures to provide constant homogenous suspension of the cells (see http://www.biocompare.com).

The here presented "Planktongravistat" is a device that constantly rotates the bottles like the many rolling devices or plankton wheels. The difference to a rolling device is that the bottles are turned very slowly (1 rpm) orthogonal to and not around or parallel to its axes. So the bottles are not turned around the liquid but the liquid is turned with the bottle. Here the working principle is not turbulence or transport in an accelerated boundary layer but the fact that the acceleration of gravity constantly changes its direction. The particle sinks or boys on the spot (in circles). The advantage is that unnatural strong small scale turbulence and shear forces that occur at the walls of the vessel are reduced. The device is suitable for eight round bottles without headspace of all types and materials up to a volume of 2.5 l. Due to the rotation in constant distance to a light source and the white design it is perfectly suitable for phytoplankton cultures. According to the sedimentation velocity of the suspended particles rotation speed is continuously adjustable between 0.5 and 5 rpm. The construction in white PVC, acryl and seawater prove stainless steel provides durability and the brushless precision gear motor assures reliability.

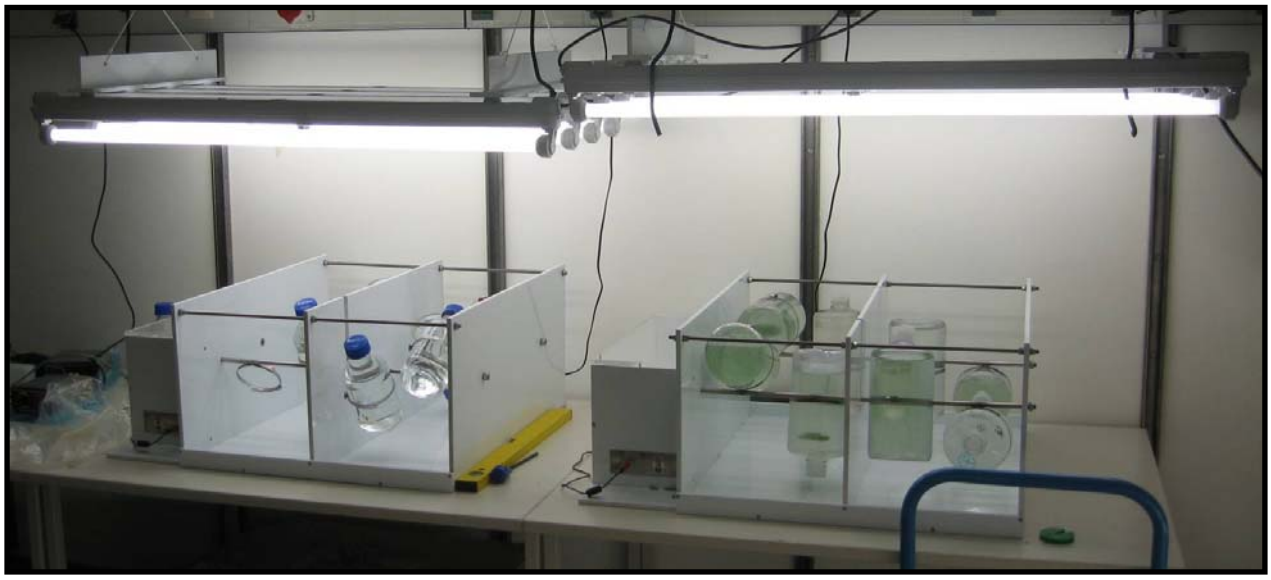

Figure 23: Planktongravistat. The two prototypes in the test phase culture growing (left). Conglomeration and re-suspension of cyanobacterial aggregates (right).

6.3.1. Verwendete Materialien

Firma:	**Conrad Elektronic Gmbh & Co.Kg**	
Anzahl	**Artikelbezeichnung**	**Best. Nr.**
1	Zahnriemenscheibe 10 Zähne	226106-WX
2	Zahnriemenscheibe 60 Zähne	226045-WX
4	Edlstahl Lager 10mm	221883-WX
1	50W Schaltnetzteil SPS 2405 5 - 24V/5 A	510500 - RT
1	Kippschalter TA201A1	700974-F4
1	Indikator Plate ein/aus	701008-7S
1	Einbaubuchsen	733954-F4
1	Kohleschichtwiederstand 6,8K	405353-7S
1	Spindeltrimmer 10K	425109-S3
1	Feinsicherungen 0,315A	551023-62
1	Sockel für Feinsicherungen	534595-82
1	Hartpapierplatine	527629-LN

Firma :	**Adolf Richter; Stahl-Metall-Kunstoffe GmbH; Kiel**	**Bunsenstr. 2A 24145 Kiel**
Anzahl	**Artikelbezeichnung**	
2	PVC Platte weiß 10mm stark 1000 x 2000 mm	
1	Acryll Glas GS Zuschnitt farblos 10mm stark 1030 x 600mm	

Firma:	Dr. Fritz Faulhaber Gmbh & Co.Kg; Schöneich	
Anzahl	**Artikelbezeichnung**	**Best. Nr.**
1	Getriebe motor 3153K024B RC32/1 308:1	990.020.000

Firma:	Franz Schoppe Industrie- und Schiffsbedarf GmbH & Co.Kg; Kiel	Grasweg 22 24118 Kiel
Anzahl	Artikelbezeichnung	
10	Selbstsichende Muttern M4 (V2A Stahl)	
22	Schrauben M4*30 /DIN 933 mit Senkkopf (V2A Stahl)	
4	Selbstsichende Muttern M10 (V2A Stahl)	
2	Gewindestange M8 (V2A Stahl)	
1	Gewindestange M4 (V2A Stahl)	
4	Selbstsichende Muttern M8 (V2A Stahl)	
8	Muttern M8 (V2A Stahl)	
12	Unterlegscheiben M8 (V2A Stahl)	
4	Unterlegscheiben M10 (V2A Stahl)	
1	Kugellager d= 10mm innen; 40mm außen	

Firma:	Gebrüder Barth GmbH & Co.Kg; Kiel	Braunstr. 34 24145 Kiel
Anzahl	**Artikelbezeichnung**	
2	Rundmatereal d=10mm V2A	
1	Endlosschellenbad SXB 2408000003	
1	Zahnflachriemen 438 XL 037 (9,5 mm breit)	

6.3.2. Konstruktionspläne

Planktongravistat
Draufsicht

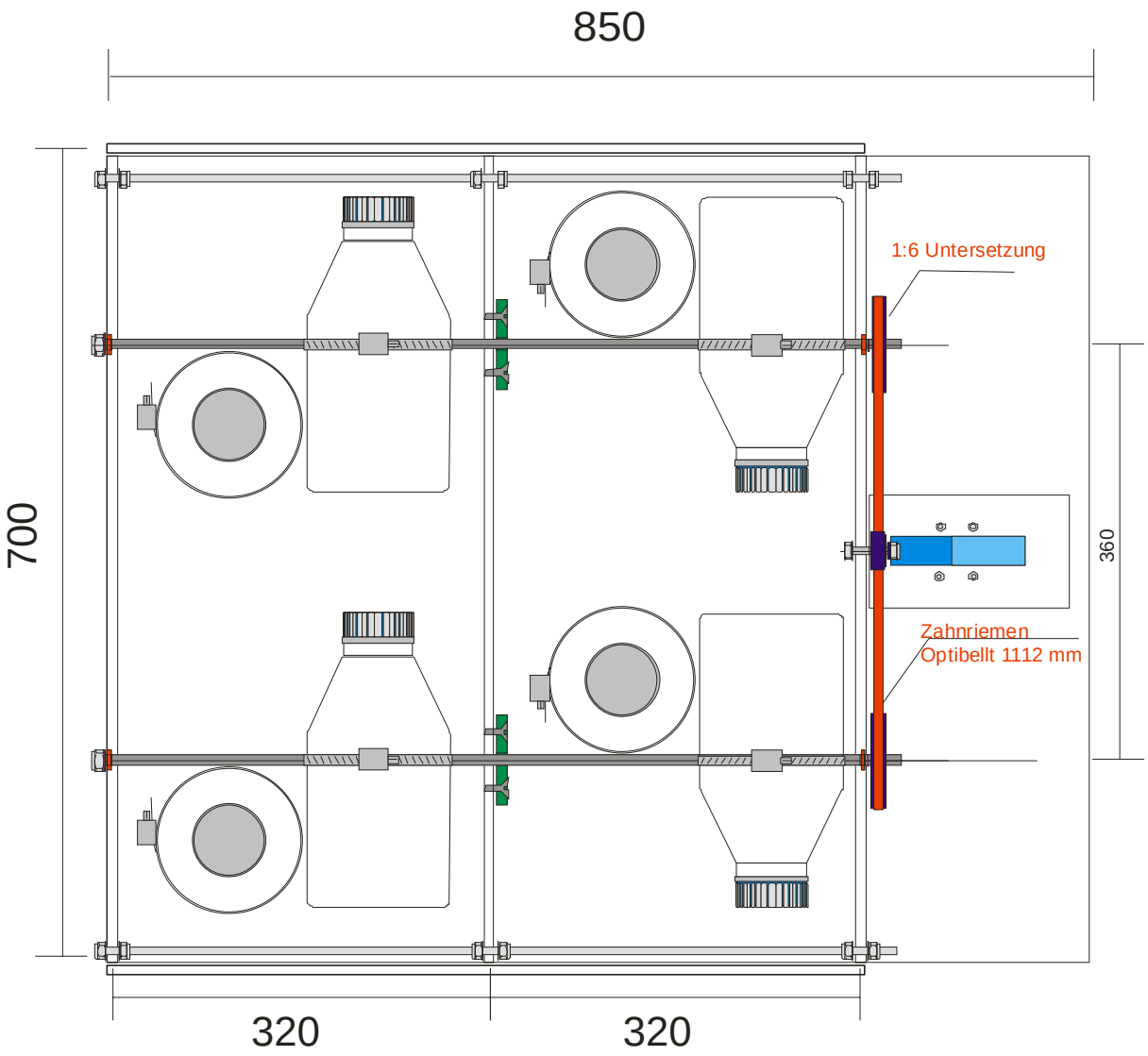

Planktongravistat
Seitenansicht

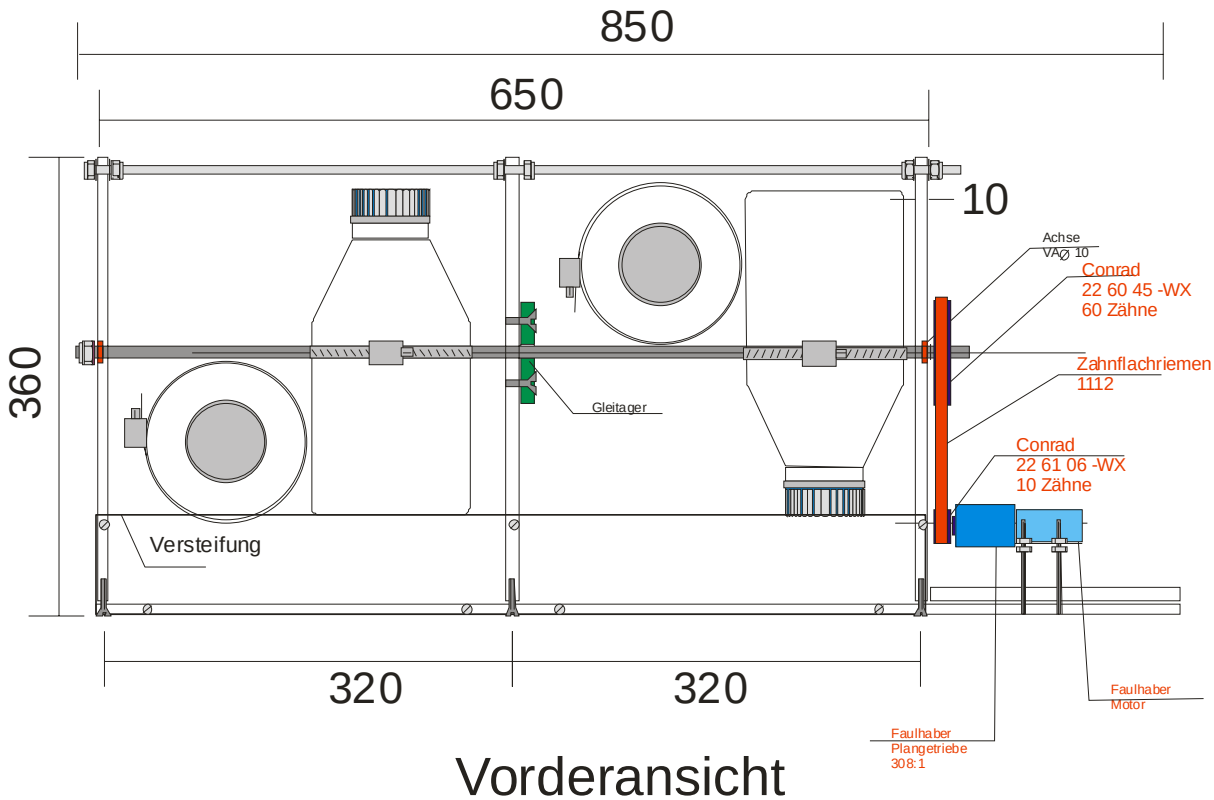

Vorderansicht

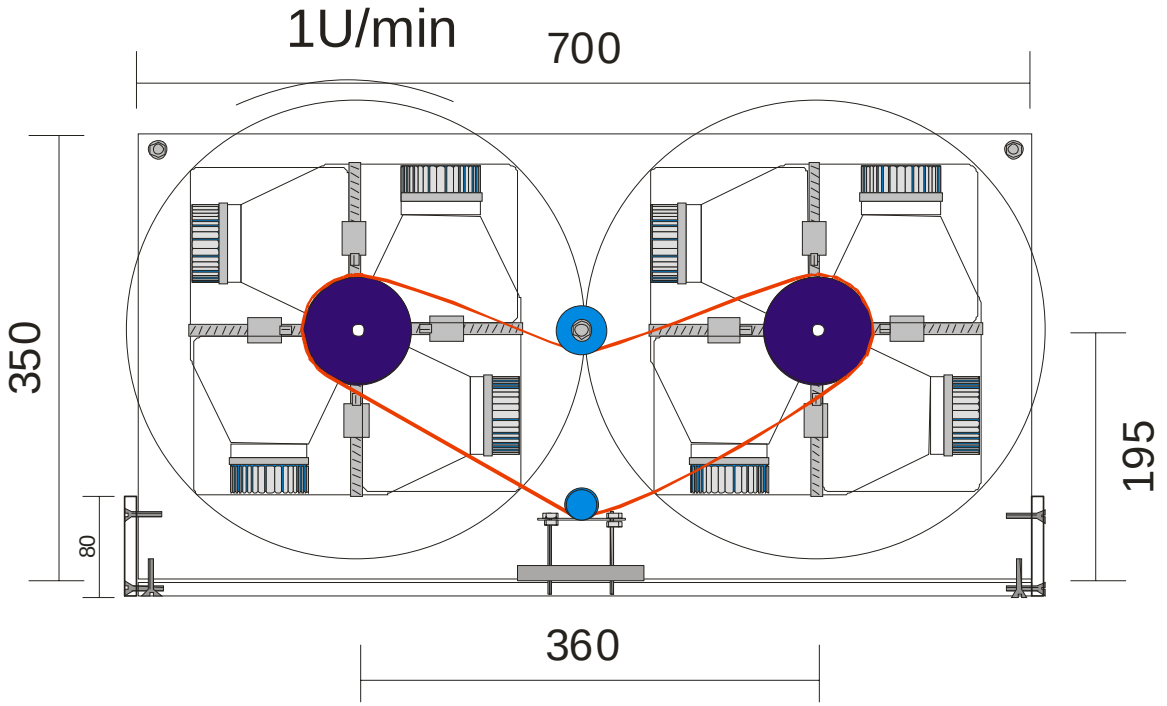

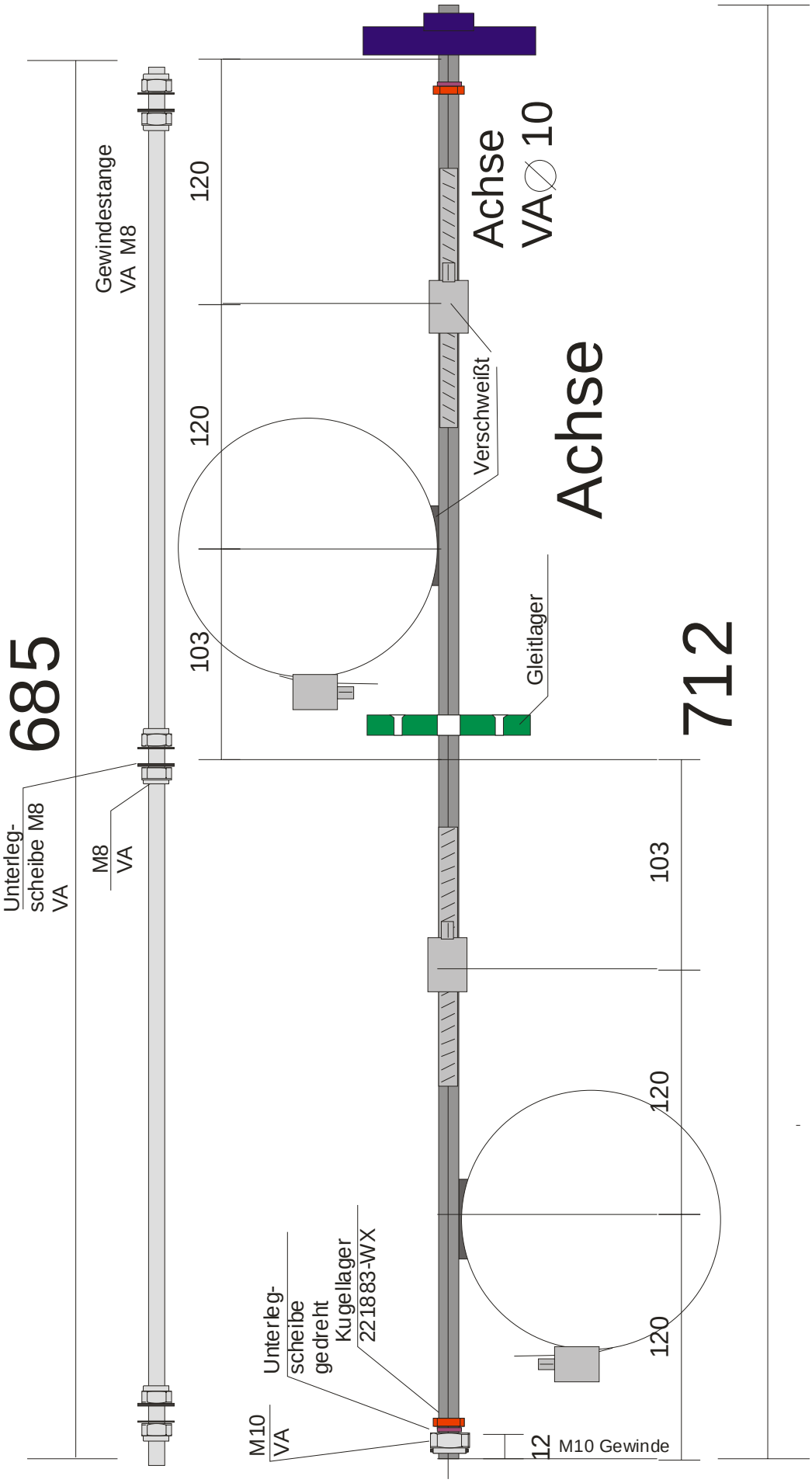
685
712
Gewindestange
VA M8
Unterleg-
scheibe M8
VA
M8
VA
120
120
103
Achse
VA∅ 10
Achse
Verschweißt
Gleitlager
103
120
120
Unterleg-
scheibe
gedreht
Kugellager
221883-WX
M10
VA
12
M10 Gewinde

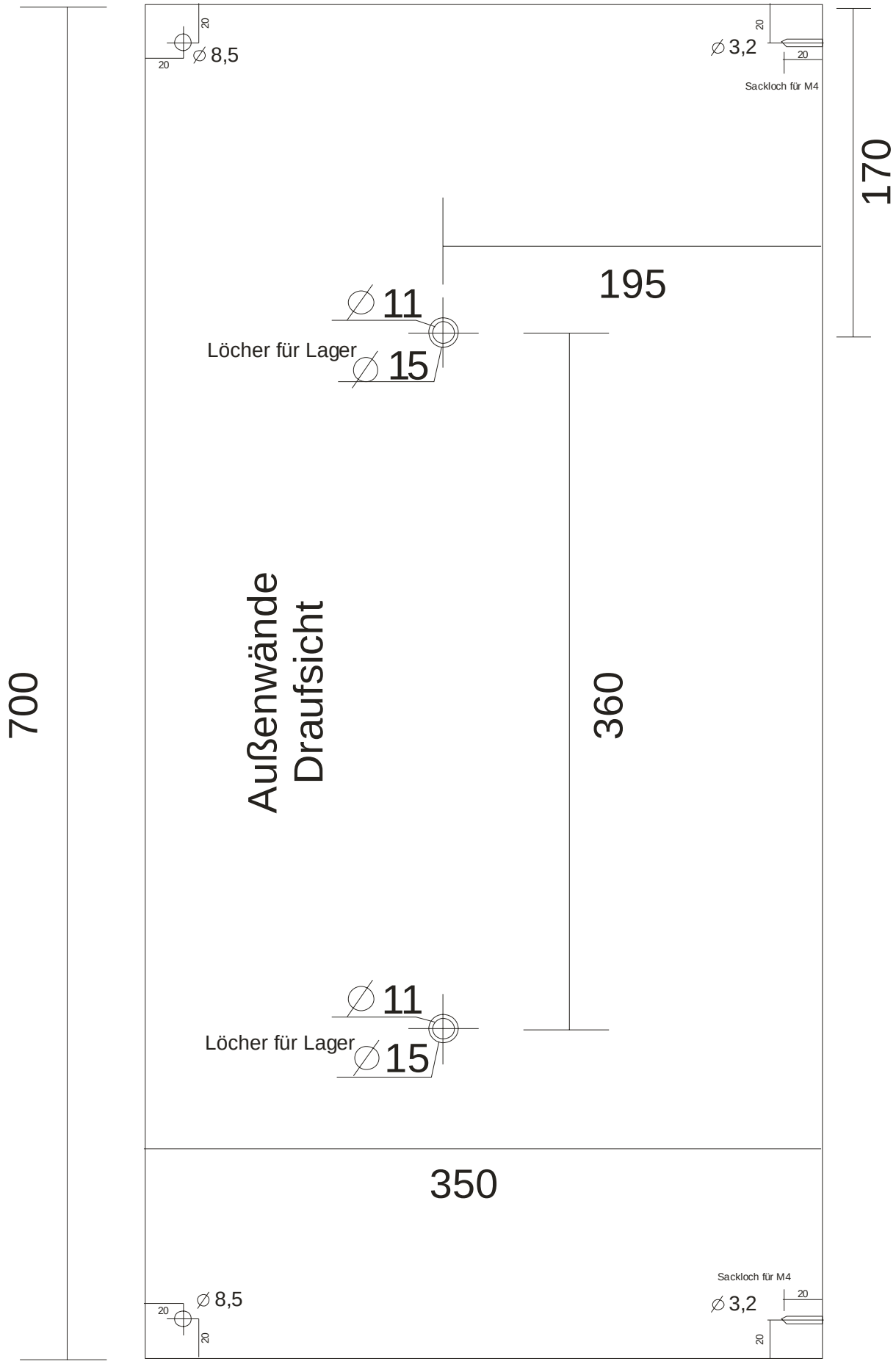
20
20
∅ 8,5
20
20
∅ 3,2
20
Sackloch für M4
170
195
∅ 11
Löcher für Lager
∅ 15
700
Außenwände
Draufsicht
360
∅ 11
Löcher für Lager
∅ 15
350
Sackloch für M4
20
20
∅ 8,5
20
20
∅ 3,2
20

Außenwände
Seitenansicht

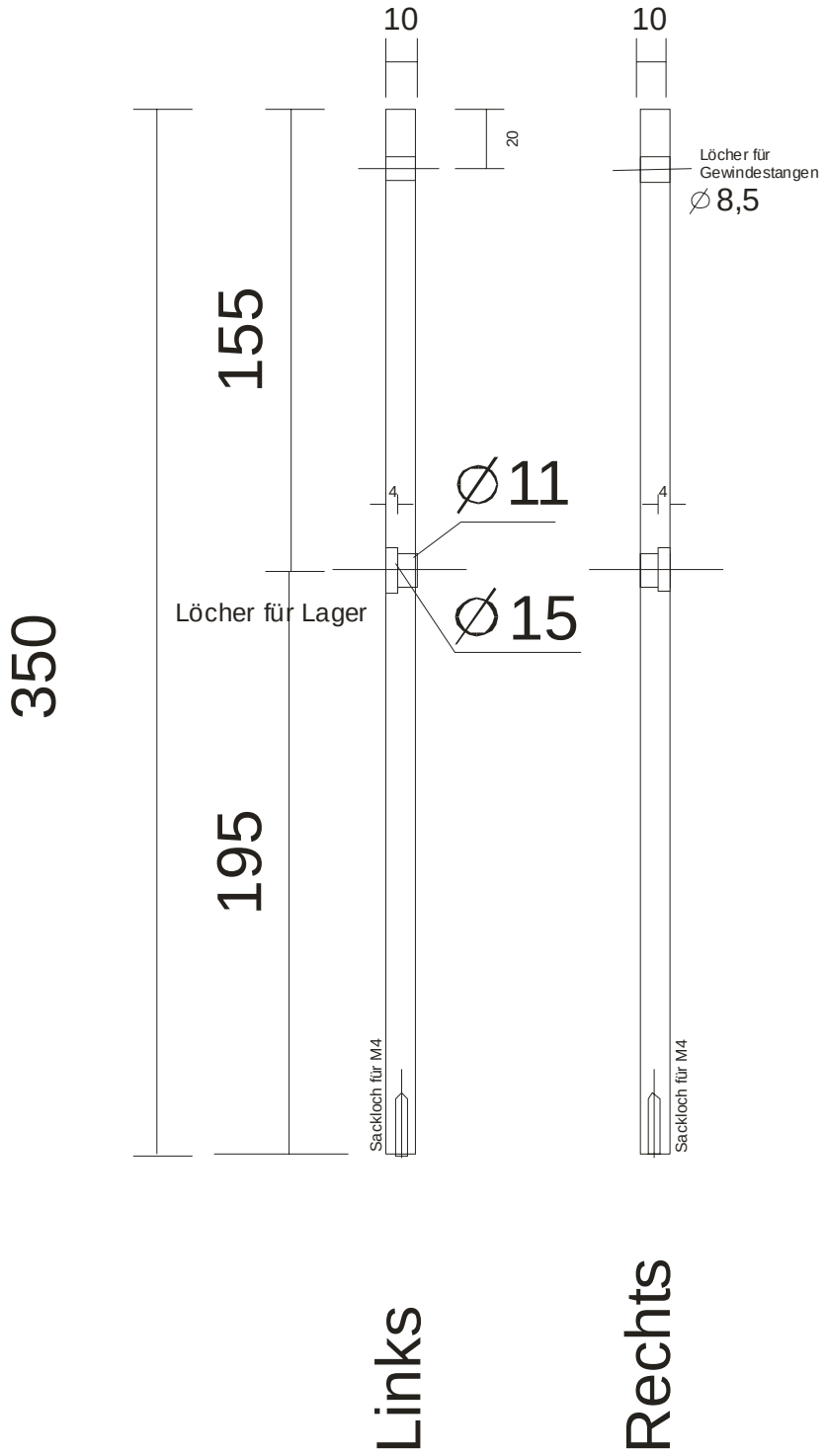

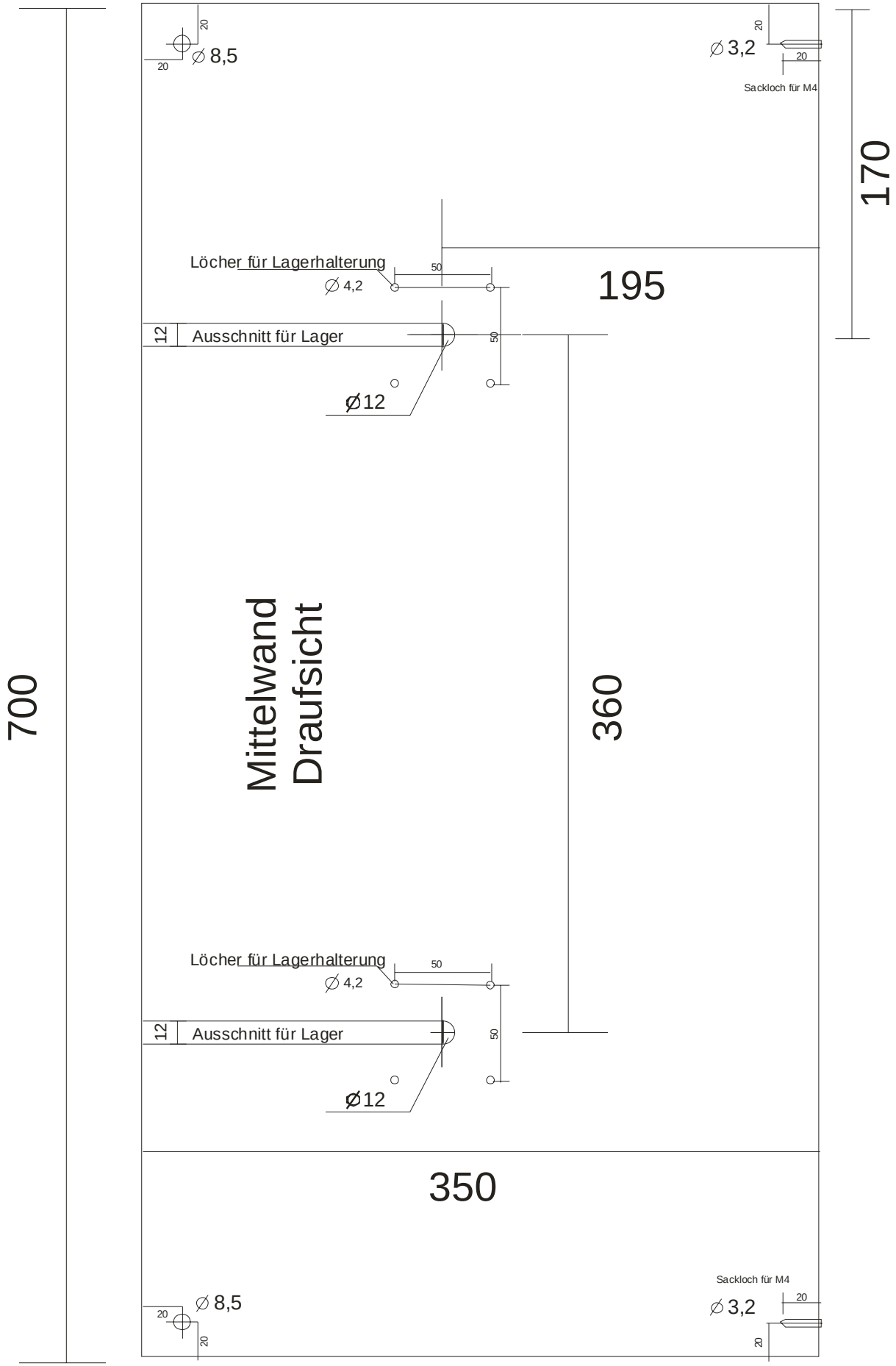
20
20
∅ 8,5
20
20
∅ 3,2
20
Sackloch für M4
170
Löcher für Lagerhalterung
50
∅ 4,2
195
12
Ausschnitt für Lager
50
∅12
700
Mittelwand
Draufsicht
360
Löcher für Lagerhalterung
50
∅ 4,2
12
Ausschnitt für Lager
50
∅12
350
Sackloch für M4
20
∅ 3,2
20
20
∅ 8,5
20
20

Mittelwand
Seitenansicht

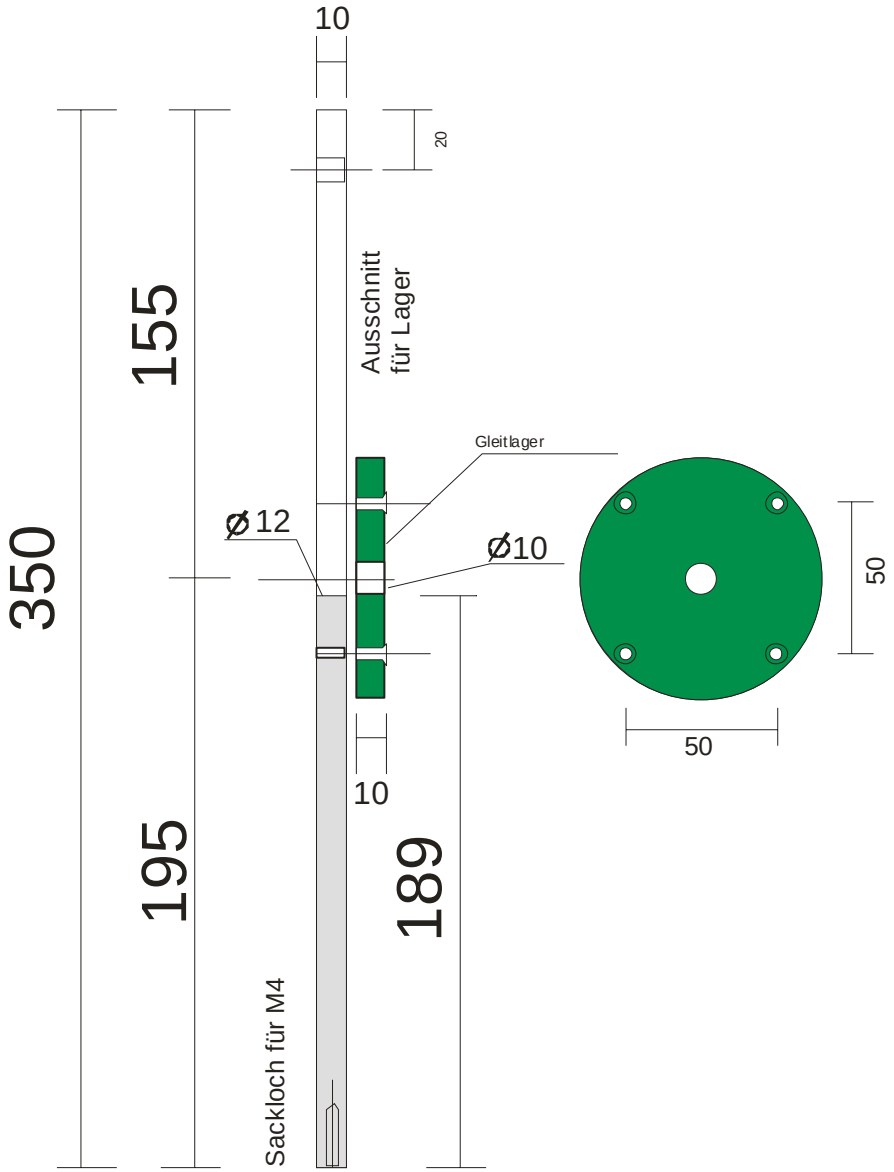

Gehäuse für Antrieb und Elektronik

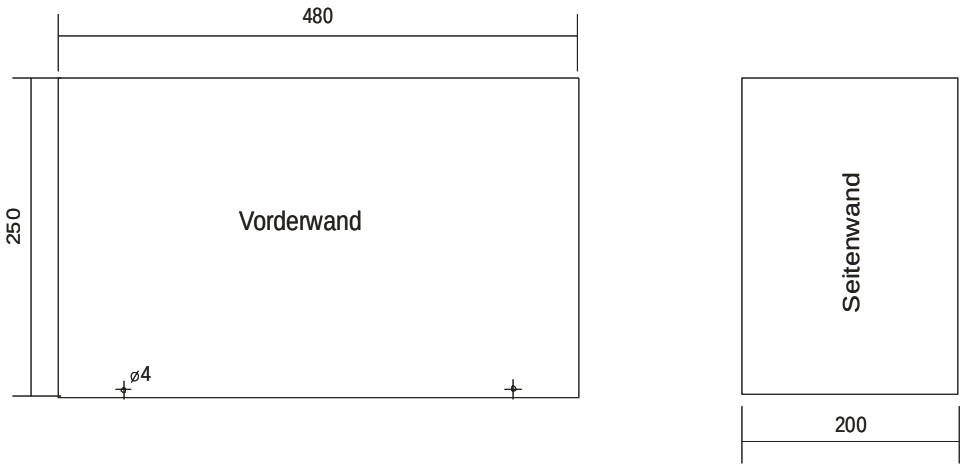

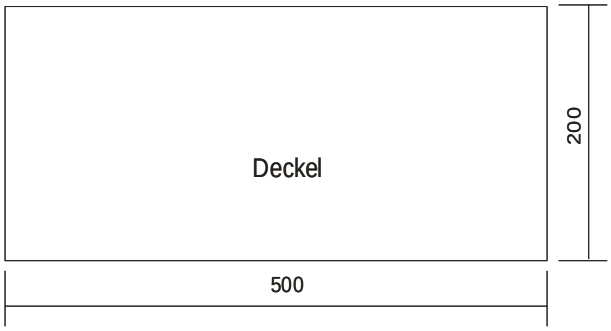

Material Plexi
Stärke 10 mm
Teile sollen verklebt werden

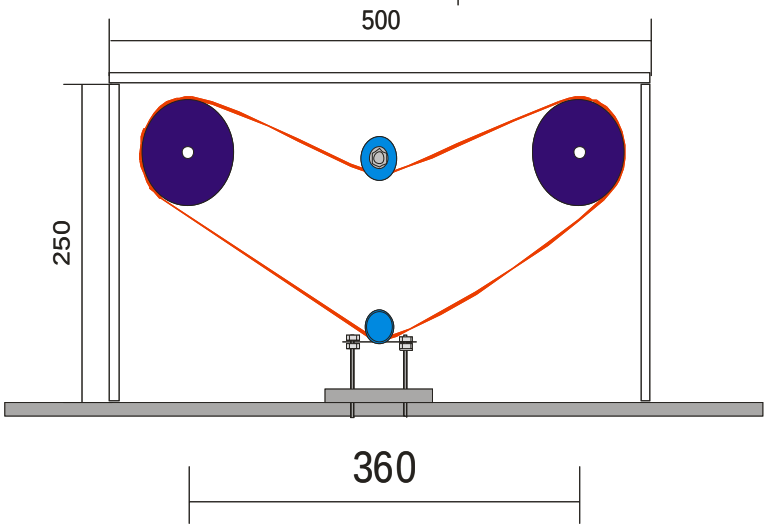

6.3.3. Schaltplan für Regelplatine

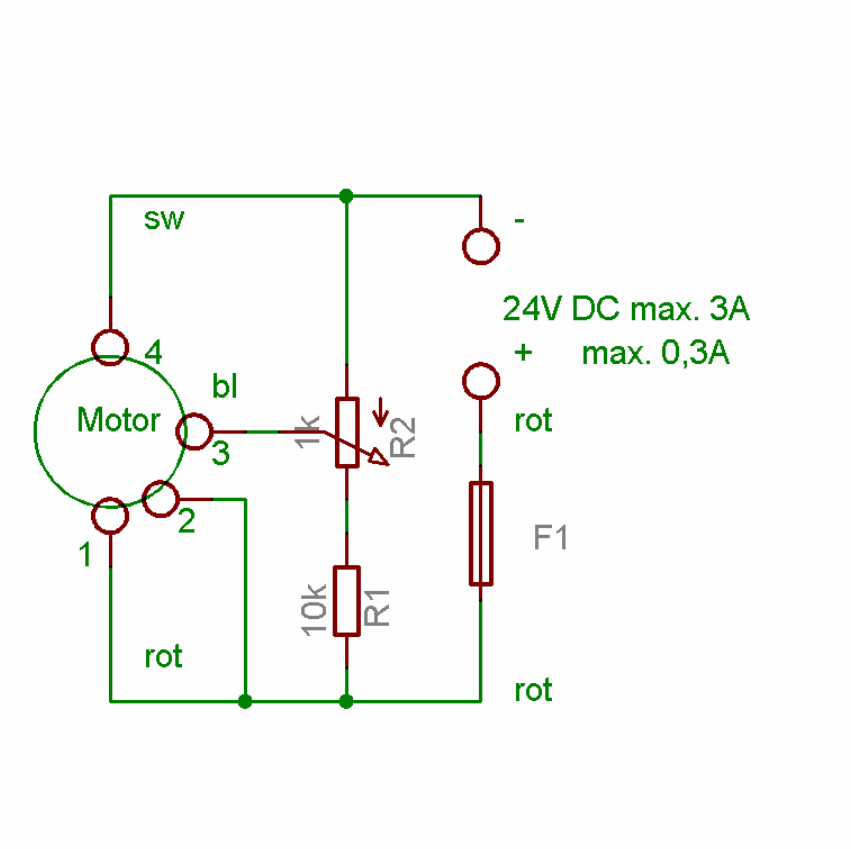

Figure 24: Wert für F1 richtet sich nach thermisch zulässigem Dauerstrom (750mA) muss aber wegen Stromspitzen in der Beschleunigungsphase sehr träge gewählt werden. Spindeltrimmer R2 ermöglicht stufenlose Drehzahlreglung.

6.3.4. Isolierreck für Stickstofffixierung (50 ml Vials)

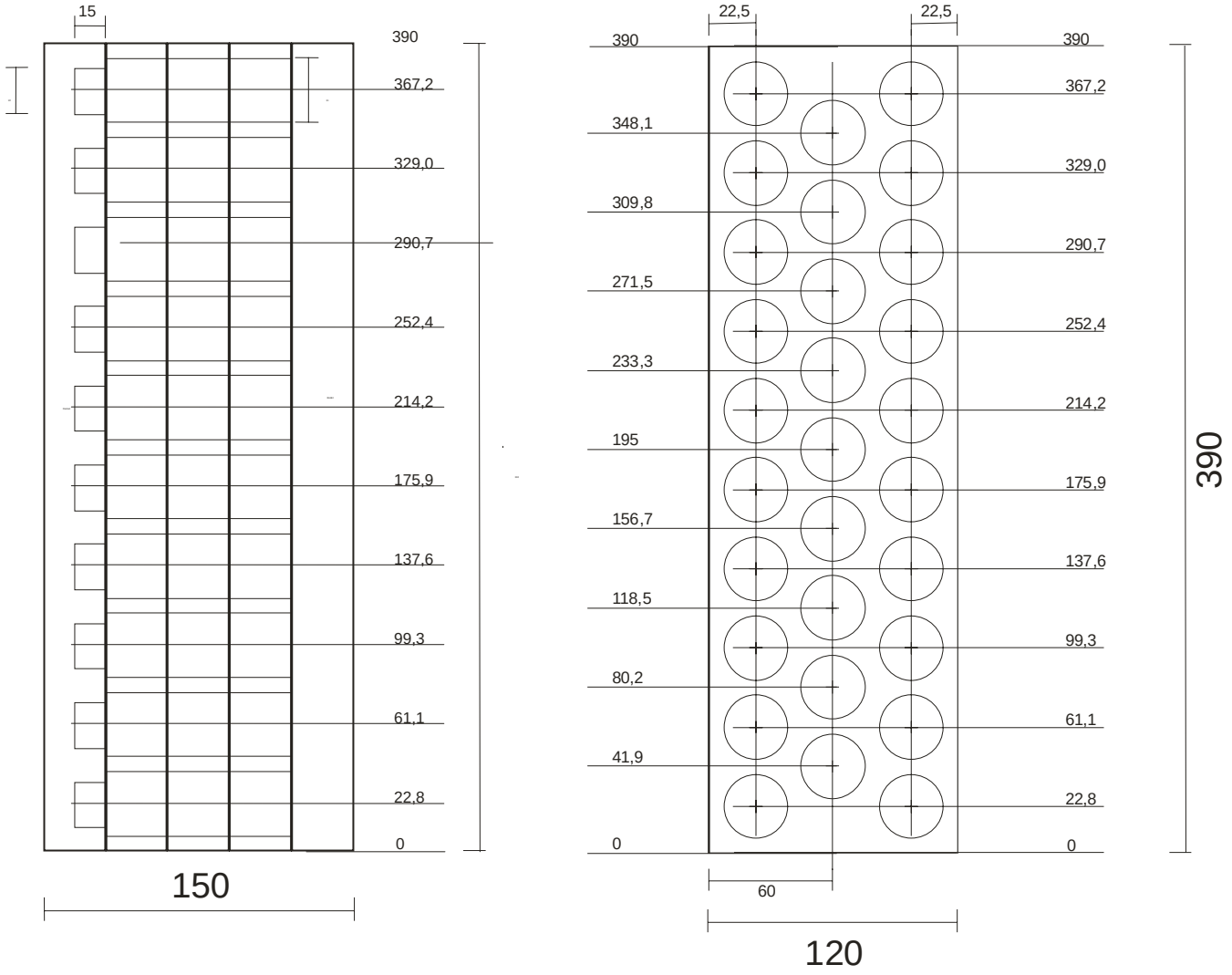

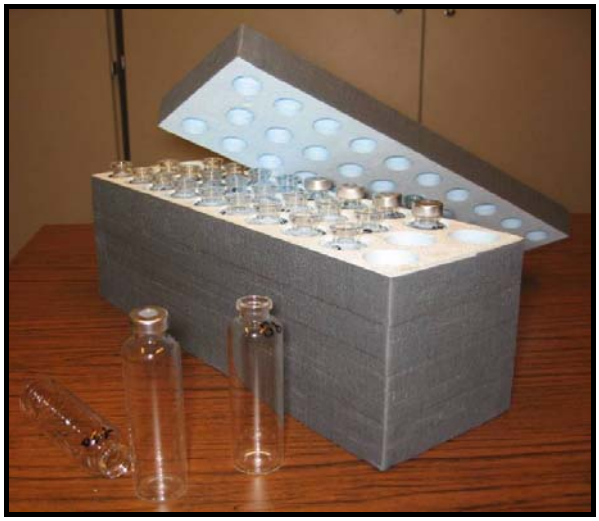

Figure 25: Das Isolierreck nimmt 29 50ml Vials auf.

6.4. The cell count method

Table 10: Settings for the 12 steps used for the Macro to convert the pictures in Adobe Photoshop 6.0 (german version) according to Manfried Dietsch

Step	Setting
1	Menü: Bild / Anpassungen / Auto-Tonwertkorrektur
2	Menü: Bild / Anpassungen / Auto-Kontrast
3	Menü: Bild / Anpassungen / Auto-Farbe
4	Menü: Bild / Anpassungen / Helligkeit/Kontrast (Helligkeit 150; Kontrast 100;)
5	Menü: Filter / Rauschfilter / Staub und Kratzer... (Radius 10; Schwellenwert 0;)
6	Menü: Filter / Scharfzeichnungsfilter / Unscharf maskieren ... (Stärke: 80%; Radius: 10; Schwellenwert: 0;)
7	Menü: Auswahl / Farbbereich (Toleranz: 200; Ausgewählte Farbe: Weiß;) die Auswahl mit der Farbe Weiß füllen
8	Menü: Auswahl / Auswahl umkehren; die Auswahl mit der Farbe Schwarz füllen
9	Menü: Auswahl / Auswahl aufheben
10	Menü: Bild / Modus / Indizierte Farbe ... (Palette: Lokal (Selektiv); Farben: 2; Erzwungen: Schwarzweiß; Transparenz: ohne; Dither: Diffusion; Stärke: 75%;)
11	Datei speichern z.B. als GIF-Grafik
12	Diesen Vorgang / diese Filtereinstellungen als Stapelverarbeitungs- Makro mit den gewünschten Grafik-Dateien durchführen.

6.4.1. Statistical discussion

The patchiness of the distribution of filaments on a filter demands for a statistical consideration of the number of photographs taken as a subsample. As it is impossible to count all filaments of a filtered sample, it is essential to count at least a number of photographs large enough to be representative for the whole filter. The histograms and the Kolmogorov-Smirnov tests of the here taken ~40 photographs per filter show in all given examples (16a, 3, 15b) (Figure 26a, 27a, 28a) that the samples do not differ significantly from

normal distribution. The sample size is large enough that the mean values taken for cell counts are representative for the whole filters. Considering the fact that the experiment had a total of 40 filters, resulting in ~1600 photographs, this would be too time-consuming to count conventionally (using the computer program Image-J). The automatic method presented here gives quick results (spreading values) that can be correlated empirically with only a few filament lengths being estimated conventionally.

Photographs of filter 16 a (see fig) were used for empirical calibration of the electronic cell count method. A factor of 540µm filament length per % spreading was calculated. As the quality of the photographs in 16 is very similar to quality of photographs in most of the other samples (1, 4-12, 16-20) the conversion factor of 540 was generally applied. Scattering in (Figure 26b) is caused by slightly varying surface of the filaments and by occasionally occurring "snow" (Figure 26).

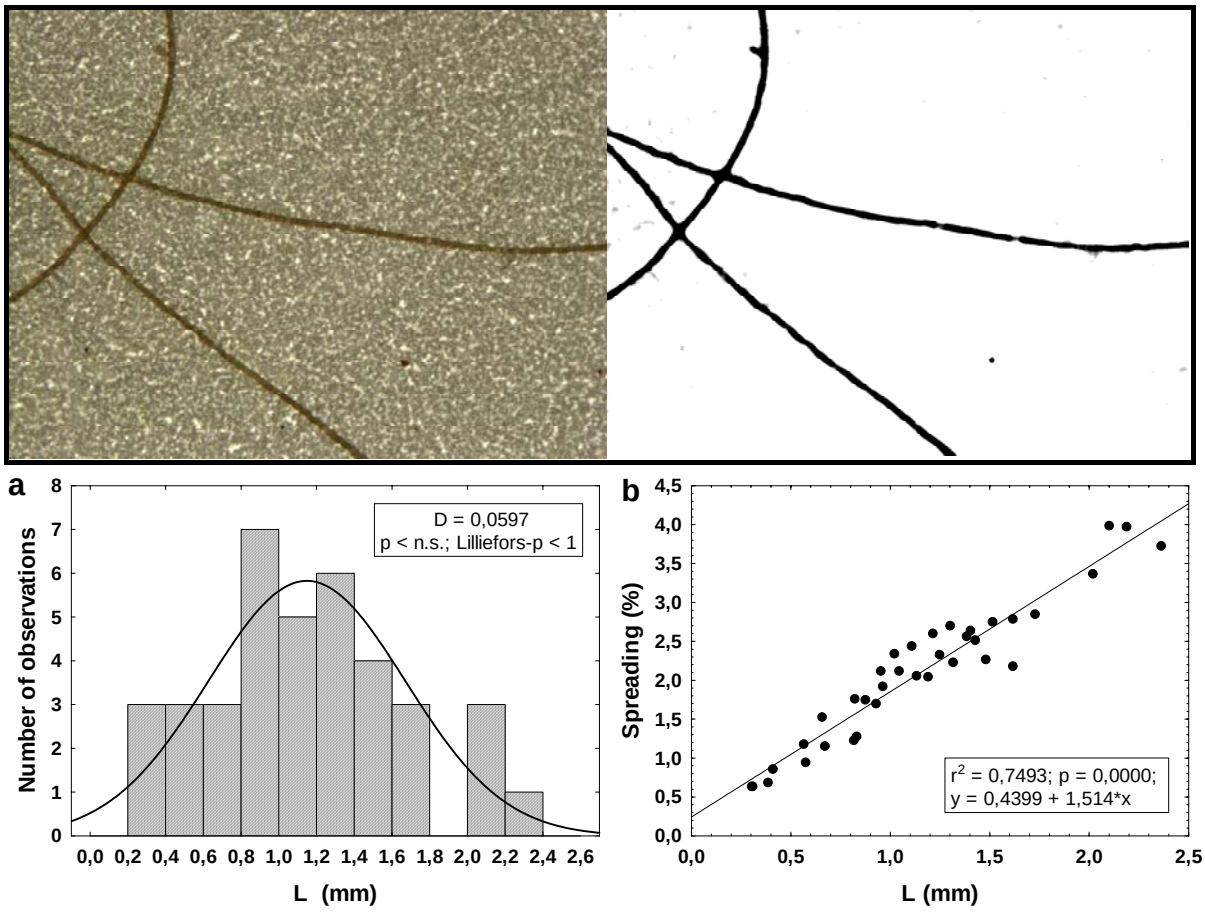

Figure 26: The microscopic photograph (left) and macro result of the photograph (right) was taken from filter a of replicate 16. Histogramm (a) shows the distribution of filament length of all measured photographs of of filter 16a with Kolmogorov-Smirnov test results for normal distribution (Box). In the scatterplot (b) the raw data of the automatic cell count method (spreading) is plotted versus manually measured filament length of the single photographs.

Samples of replicate 1 and 3 of the lowest CO_2 treatment were the first samples of the experiment to be photographed. The microscope and camera settings differed from those used

in the pre-cultures (i.e. 16a), resulting in a pitted looking background with quite strong contrast patterns (Figure 27). These contrast patterns beside the filaments caused underestimation of filament surface on the one hand and "snow" in the background on the other. Combined results of that are a much stronger scattering of data (Figure 27b) and a slight systematic underestimation of cell numbers (Figure 29).

This systematic error was not as large as to alter strong effects like in growth rate or C/Cell but the influence on relatively weaker effecs like N/Cell (Figure 9b) and nitrogen fixation/cell (Figure 13) or chl a/cell (Figure 9c) was stronger (the data points 1, 3 were marked (open circles)).

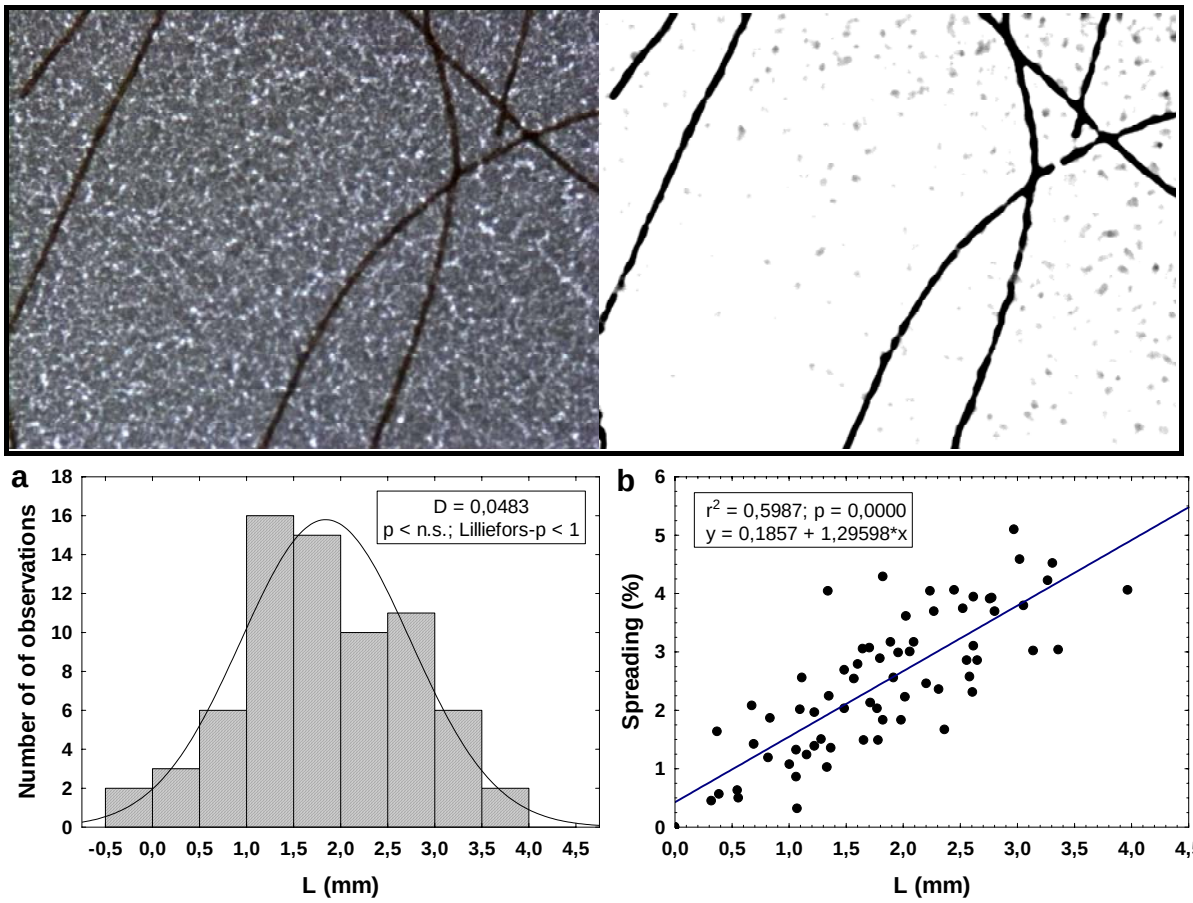

Figure 27: The microscopic photograph (left) and macro result of the photograph (right) was taken from a filter of replicate 3. Histogramm (a) shows the distribution of filament length of all measured photographs of filter 3 with Kolmogorov-Smirnov test results for normal distribution (Box). In the scatterplot (b) the raw data of the automatic cell count method (spreading) is plotted versus manually measured filament length of the single photographs.

Samples of replicate 14 and 15 of the highest CO_2 treatment were the last samples of the experiment to be photographed. When focussing on filter 14 a finally a setting was found that provides perfect contrast properties for the automatic cell count method (Figure 28b). The filaments on the photographs (Figure 28) on the left side are represented by thick black lines

on a pure white background on the right side after the macro was applied. However the filaments are slightly overrepresented compared to the calibration (Figure 29).

This systematic error is even smaller than the one of replicate 1 and 3 but can at least partly explain the offset of the two marked data points (open circles) in the high CO_2 area of Figure 8, 9 and 13. Anyway this systematic difference was the reason for marking the points. The offset in these points could have been corrected for by using an adapted factor based on the here presented conventional counting. But consequently only one factor was used because the individual correction of the marked data points would have demanded for verification of all datasets.

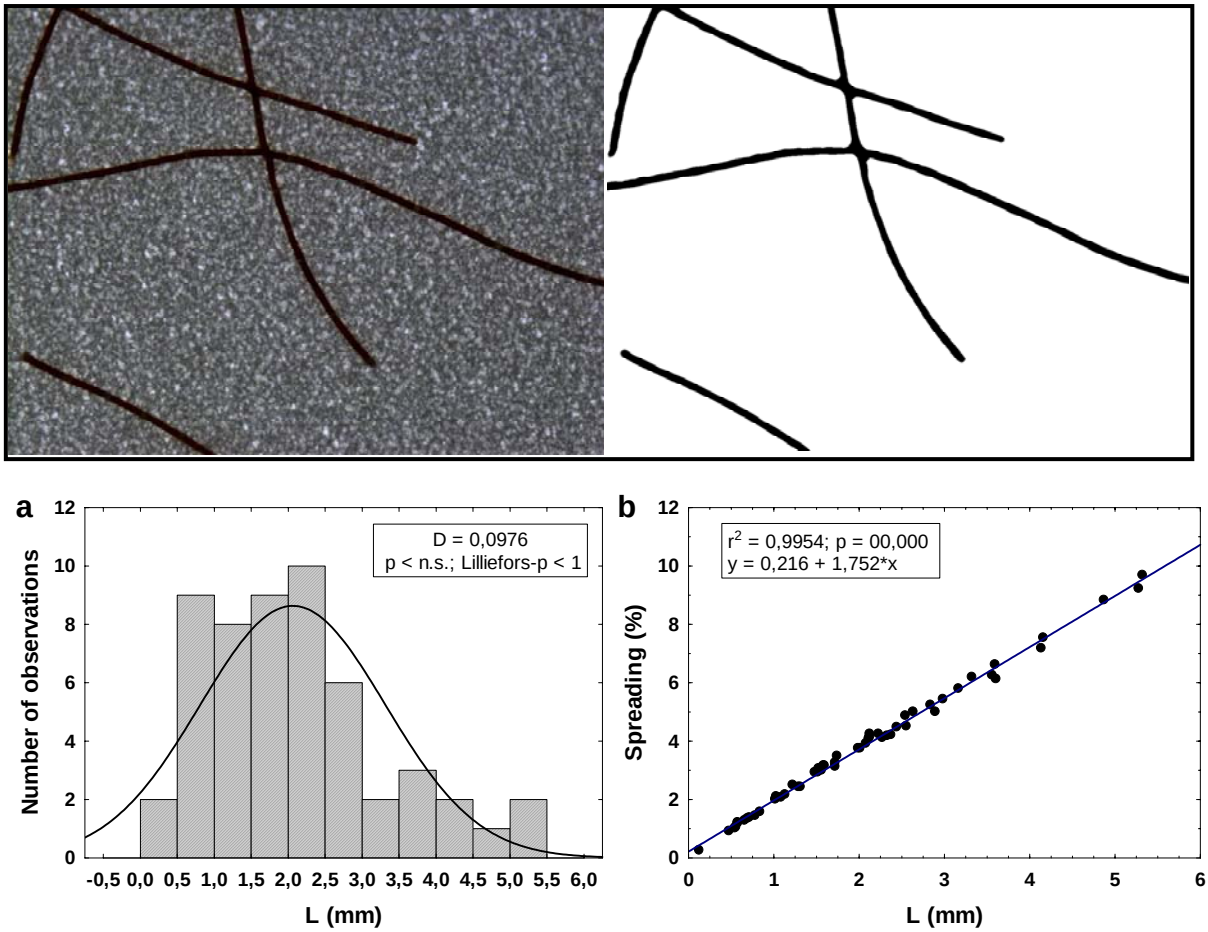

Figure 28: The microscopic photograph (left) and macro result of the photograph (right) was taken from filter b of replicate 15. Histogramm (a) shows the distribution of filament length of all measured photographs of filter 15b with Kolmogorov-Smirnov test results for normal distribution (Box). In the scatterplot (b) the raw data of the automatic cell count method (spreading) is plotted versus manually measured filament length of the single photographs.

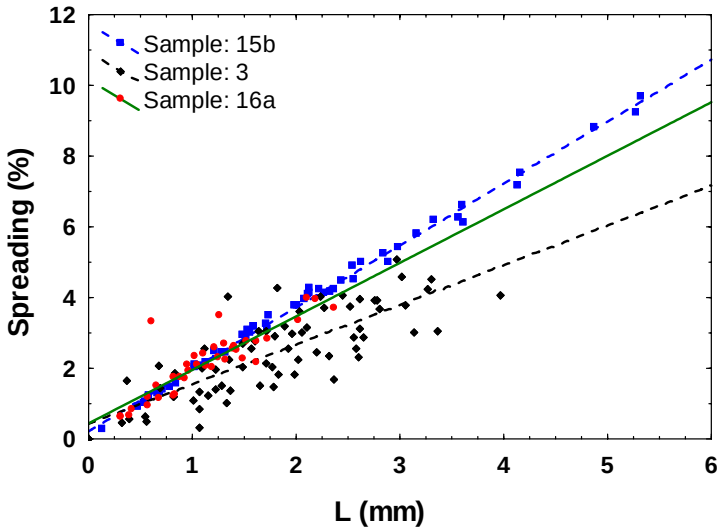

Figure 29: The scatterplot shows the raw data of the automatic cell count method (spreading) plotted versus manually measured filament length of the single photographs of the filter 3, 15a, 16a.

Based on the experience made in this experiment much more precise cell count data can be achieved with this method in future works. Attention should be paid that the photographs have all contrast and colour properties like in Figure 28.

7. Danksagung

Zuerst möchte ich Joana Barcelos e Ramos danken, die mir immer zur Klärung und Diskussion von Fragen und methodischen Probleme zur Verfügung stand und sich auch auf meine teilweise recht unkonventionellen Ideen eingelassen hat.

Einen herzlichen Dank an Prof. Dr. Ulf Riebesell für die konstruktive Kritik an meiner Arbeit und das Vertrauen in meine technischen Fähigkeiten, so dass er mir etliche Beschaffungsanträge mit diversen Bauteilen bewilligte.

Besonderen Dank an Paul Debes und Kathrin Bremer und noch einmal an Joana für die intensive Lektüre der Rohfassungen meiner Arbeit, Paul auch für die Hilfe bei verschiedenen Computer- und Statistikproblemen und dafür, dass er immer ein offenes Ohr für überhaupt alles hat.

Dank auch an Richard Knight Jesse Bonwit und Michael Müller für Antworten aus erster Hand, betreffend Fragen des korrekten englischen Ausdrucks.

Besonderen Dank schulde ich Manfried Ditsch, der mit mir die elektronische Zellzählmethode entwickelt hat, mehrmals das Makro umschreiben und umfassende Erörterungen über Bakterien über sich ergehen lassen musste (nicht leicht für einen Informatiker !).

Peter Fritsche danke ich für die Einweisung in chemische Analysen und die Hilfe bei der Durchführung, Kerstin Nachtigall für C/N Analysen und Dr. Michael Meyerhöfer für DIC Analysen.

Einen ausdrücklichen Dank auch dem gesamten Team des Technik - und Logistikzentrums und hier besonders Roland Muche für die Hilfe bei Arbeiten um die Konstruktion des Planktongravistats, aber vor allem auch dafür, dass man mich in dieser tollen Werkstatt so selbständig hat arbeiten lassen.

Vielen Dank an Jasmin Franz, Sebastian Krug und Marius Müller dass sie ihren Erfahrungsschatz, was planktologische Methoden angeht, mit mir geteilt haben, besonders danke ich Sebastian für die professionelle Hilfe bei den endlosen Filtrationsarbeiten am Probennahmetag.

Außerdem danke ich Dr. Kai Schulz für bereitwillige Hilfe, wenn sich die Karbonatchemie wieder mal von ihrer rätselhaften Seite gezeigt hat.

Last but absolutely not least kann ich meinen Eltern nicht genug danken, die mich nicht nur während meines gesamten Studiums von allen finanziellen Sorgen frei gehalten haben, sondern mich grundsätzlich wohlwollend in allem unterstützen, was ich vorhabe. Expliziten Dank an meinen Vater, der mich schon sehr früh für die Naturwissenschaften begeistert hat

und als Ingenieur und Chemiker auch während der Diplomarbeit ein wertvoller Diskussionspartner war.

8. Eidesstattliche Erklärung

Hiermit bestätige ich, dass die vorliegende Arbeit mit dem Titel:

Influence of future CO_2 concentrations on growth and nitrogen fixation in the bloom-forming Cyanobacterium *Nodularia spumigena*

von mir selbständig verfasst worden ist und keine weiteren Quellen und Hilfsmittel als die angegebenen verwendet wurden.
Ich erkläre mich damit einverstanden dass diese Arbeit an die Bibliothek des IFM-Geomar und die Universitätsbibliothek der CAU weitergeleitet wird.

_____

Jan Czerny